The generation, diffusion, spin motion, and recombination of radical pairs in solution in the nanosecond time domain

Z. Schulten and K. Schulten

Max-Planck-Institut für Biophysikalische Chemie, Abteilung Spektroskopie, 34 Göttingen, Federal Republic of Germany
(Received 3 September 1976)

Pairs of radical ions generated in polar solvents by photoinduced electron transfer either recombine within a few nanoseconds to singlet and triplet products or separate. On the basis of recent time-resolved observations of a magnetic field dependence of the pair recombination a theoretical description of this process is provided. The description, similar to the radical pair theory of CIDNP and CIDEP, is founded on a coherent spin motion superimposed on the diffusive motion of the radicals. The spin motion is induced by the hyperfine coupling between electron and nuclear spins and can be modulated by low (0–200 G) magnetic fields. The spin-selective recombination of radicals is accounted for by a Feshbach optical potential. The diffusion process described by a Smoluchowski operator depends sensitively on the solvent properties. For the case of free Brownian motion, simple analytical expressions for the time- and magnetic-field-dependent recombination yields are derived. For the Brownian motion of oppositely charged radical ions a differential–difference approximation is used to demonstrate the dependence of the recombination yields on the viscosity and polarity of the solvent medium as well as on the strength of the hyperfine coupling and on the rate of the electron back transfer.

I. INTRODUCTION

Observations of elementary reaction processes have in the past been mainly confined to the gas phase. The advent of short time laser methods makes it feasible, however, to monitor elementary reaction processes also in the liquid phase with a nanosecond time resolution. From observations of reaction events in the gas phase, an understanding of reaction dynamics governed by the reactant–product potential surfaces has evolved. Clearly, one expects that reactions in solution are much influenced by the solvent environment of the reacting particles. The solvent modifies the reactant–product potential surface and also alters the translational and rotational motion of the reactants from straight trajectories of a classical mechanical description to zig-zag random flight trajectories of a statistical mechanical description. It is this second aspect of reactions in liquids, the random motion of two reactants described by their time-dependent pair correlation function, that we want to study in this paper.

In general, the recombination of radical pairs is governed by the alignment of the unpaired electron spins (singlet or triplet) which is expressed in terms of a spin density matrix. The recombination rate and the partition of singlet and triplet products depends on the product of the pair correlation function and the spin density matrix. Once the spin density matrix is known, a time-resolved measurement of the recombination process could yield the time evolution of the pair correlation function. In the light of the recent time-resolved observation of radical recombination presented in Ref. 1, we want to point out in this paper some properties of the time-dependent pair correlation function and factors influencing it as well as the singlet and triplet recombination yields.

Let us first summarize the results of the experiments presented in Ref. 1, in which radical ion pairs were generated in polar solvents via photoinduced electron transfer between suitable acceptor and donor molecules by nanosecond laser flashes. In the case of the sample system, pyrene (Py) and 3,5-dimethoxy-*N*,*N*-dimethylaniline (DMDMA) in methanol, the radical ion pair recombines to the triplet state as well as to the ground state. The ions and their recombination products can be monitored with a nanosecond time resolution. One finds that the recombination proceeds on two different time scales. Either, the original pairs recombine directly within several nanoseconds (*first-order, geminate recombination*), or the pairs diffuse apart and recombine with members of different pairs (*second-order, homogeneous recombination*) over the time range 10^3–10^4 ns, depending on the concentrations ($\sim 10^{-4}$–10^{-5} mol dm^{-3}).

Since the radical ion pairs are being generated from singlet precursors, their unpaired electron spins are in a singlet state initially. For the recombination to the triplet state to occur the radicals must be brought to a triplet spin alignment. When radicals of different initial pairs encounter each other, the spin alignment is random, i.e., 25% of them encounter in a singlet and 75% in a triplet alignment. The appearance of triplet recombination products after a long time ($\sim 10^3$ ns) is then readily explained. However, triplet recombination products appear already in the early geminate phase of the recombination process. The mechanism by which the spin multiplicity of the radical ion pairs is changed within the short time of a few nanoseconds has been the subject of much debate. It was first suggested by Brocklehurst[2] and more recently by Orbach and Ottolenghi[3] that the fast spin multiplicity changes may be caused by the hyperfine coupling between unpaired electron and nuclear spins.

The hyperfine coupling induces transitions between the degenerate S_0 and T_0, T_{+1}, T_{-1} electron spin states of the radical pairs. An external magnetic field, however, lifts the degeneracy between the S_0, T_0, and the $T_{\pm 1}$ states. For field strengths of the order of the hyperfine coupling constant the transition probabilities

between these states and, consequently, the triplet product yield, will be reduced. As a magnetic field effect is not to be expected for the long time (10^3 ns) recombination process involving radicals of different initial pairs, the magnetic field effect separates out the geminate recombination. It has been reported in Ref. 1 that the triplet yield of recombining radical ion pairs in polar solvents is reduced by weak (0–100 G) external magnetic fields. In a time-resolved experiment the magnetic field effect was demonstrated to build up over the geminate phase of the recombination process. The magnetic field dependence of the triplet yield was found to be in agreement with the prediction of a theoretical model based on the hyperfine mechanism of geminate radical recombination. Recently, Michel-Beyerle *et al.*[4] have also observed a magnetic field dependence of the geminate triplet production with a donor–acceptor system similar to that in Ref. 1.

The theoretical analysis shows that a few nanoseconds are needed for the hyperfine interaction to bring the radical ion pairs to the triplet state.[1] If the radical pairs separate much faster, the hyperfine mechanism would not be effective and no triplet products and magnetic field effect would be observed. As a magnetic field effect is observed, however, the time of the diffusive separation of the radical pairs must be of order 1 ns. The experimental measurement of the magnetic field effects on the nanosecond recombination processes provides a monitor on the diffusive motion and interaction dynamics of particles reacting in a real fluid, and therefore, may serve as a much demanded check of theoretical descriptions of this motion. It is actually possible to employ the magnetic field effect on geminate processes as a probe for quite a variety of diffusion processes, e.g., for two-dimensional membrane or liquid crystal systems or for intramolecular polymer diffusion processes.

In a first presentation of the magnetic field effect on geminate radical processes we have treated in detail the hyperfine induced spin motion of radical pairs and its modulation by an external magnetic field. The diffusive separation and the recombination reaction were modeled by a first-order kinetic scheme. Here we shall describe the diffusion process of the radical pairs during the geminate recombination phase in full detail. Leaving the formulation of the electron–nuclear spin motion intact, the Liouville equation of Ref. 1 will be replaced by a stochastic Liouville equation containing a diffusion operator of the Smoluchowski type which includes the effect of the dissipative motion arising from the force field between the recombining radicals. Such an approach has been employed before for the description of the CIDNP and CIDEP effects by Deutch,[5] by Evans *et al.*,[6] and by Pedersen and Freed[7] in a series of papers which much inspired our work. The existence of a chemical reaction will be introduced into the Liouville equation by means of a Feshbach optical potential.[8(a)] In Sec. II we will set up the theoretical framework for the description of spin-selective geminate recombination of radical pairs. In Sec. III we will determine the Feshbach optical potential in terms of second-order rate constants which are well-known experimental quantities. In Sec. IV we present an analytical treatment for the magnetic field modulated, hyperfine induced recombination of neutral radicals that are assumed to undergo free Brownian motion. Though somewhat unrealistic, the free Brownian motion description bears all essential features of the geminate recombination process. The Liouville equation for the geminate recombination of radical *ions* cannot be solved analytically and, hence, we present, in Sec. V., a numerical treatment of ion recombination processes. In particular, the effect of solvent viscosity and polarity and the hyperfine coupling strength of the geminate yield will be investigated. In Sec. VI we add some concluding remarks regarding a theoretical analysis of experimental data on time- and magnetic-field-dependent recombination yields.

II. STOCHASTIC LIOUVILLE EQUATION FOR GEMINATE RECOMBINATION

Hyperfine coupling and diffusion act in concert inducing recombination of radical pairs. For spin-selective geminate recombination the cooperation of diffusion and electron–nuclear spin interaction will be given now a theoretical formulation which lends itself to calculations of recombination rates as observed in Ref. 1.

The space, time, and electron–nuclear spin distribution of radical pairs is described by the density matrix $\rho(\mathbf{r}, t)$. The diagonal elements $\rho_{ii}(\mathbf{r}, t)d\mathbf{r}$ represent the concentration of radical pairs in some electron–nuclear spin state $|i\rangle$ in the volume element $d\mathbf{r}$ at separation $\mathbf{r}$ and at time t. The total concentration of radical pairs at time t is $\langle\rho(t)\rangle = \int d\mathbf{r}\,\mathrm{tr}\rho(\mathbf{r}, t)$ ($\mathrm{tr}\rho = \sum_i \rho_{ii}$). The density matrix is the solution of the stochastic Liouville equation

$$\frac{\partial}{\partial t}\rho(\mathbf{r}, t) = l(\mathbf{r})\rho(\mathbf{r}, t) - \frac{i}{\hbar}[H, \rho(\mathbf{r}, t)] - U(\mathbf{r})\rho(\mathbf{r}, t) - \rho(\mathbf{r}, t)\,U(\mathbf{r}) - k\langle\rho(t)\rangle\rho(\mathbf{r}, t). \tag{2.1}$$

The first term on the right-hand side (rhs) describes the relative diffusion of the radical pair. For neutral radicals one may assume the pair to undergo free Brownian motion, in which case the stochastic operator $l(\mathbf{r})$ is

$$l(\mathbf{r}) = D\nabla^2, \tag{2.2}$$

where $D = D_1 + D_2$ is the sum of the diffusion coefficients of the two radicals constituting the pair. In taking the relative diffusion coefficient D to be independent of the separation r we neglect any hydrodynamic effects[9] on the motion of the radicals. If radicals in solution are subject to a force field $\mathbf{F}(\mathbf{r})$, the diffusion may be described by the classical Smoluchowski theory[10] ($\beta = 1/kT$)

$$l(\mathbf{r}) = D\nabla \cdot [\nabla - \beta\mathbf{F}(\mathbf{r})]. \tag{2.3}$$

Operator (2.3) has the property that in a reaction-free system $\rho(\mathbf{r}, t)$ relaxes at long times to the Boltzmann distribution, i.e.,

$$\lim_{t\to\infty}\rho(\mathbf{r}, t) \sim \exp[-\beta V(\mathbf{r})], \tag{2.4}$$

where $\mathbf{F}(\mathbf{r}) = -\nabla V(\mathbf{r})$. Since the solutions of radical ions in the magnetic field experiments[1] are dilute, ($\sim 10^{-5}$ mol dm^{-3}), we take $\mathbf{F}(\mathbf{r}) = -(e^2/\epsilon r^3)\mathbf{r}$, where ϵ is the *macroscopic* dielectric constant of the medium which may be taken to depend on r in order to account correctly for the dielectric screening over microscopic distances (see Sec. III). The case when Debye–Hückel interactions are included in $\mathbf{F}(\mathbf{r})$ has been investigated by Hwang and Freed.[11]

A stochastic operator can also be employed that describes two-dimensional diffusion processes[5] as may be realized in membranes or liquid crystals. It may further describe one-, two-, and three-dimensional conduction in crystals as would be required to represent the experiments of Groff *et al.*[12] or to assess the existence of photoinduced charge separation and recombination in chlorophyll assemblies of bacteria and plants.[13] An interesting extension would also be the study of hyperfine induced recombination of biradicals, e.g., biradical polymers, in which case the stochastic operator l has to describe an intramolecular motion.

The second term of Eq. (2.1) describes the electron–nuclear spin motion of the radical pair. This motion is governed by the Hamiltonian

$$H = \sum_k a_{1k}\mathbf{S}_1 \cdot \mathbf{I}_k + \sum_l a_{2l}\mathbf{S}_2 \cdot \mathbf{I}_l + \mu\mathbf{B} \cdot (g_1\mathbf{S}_1 + g_2\mathbf{S}_2) + J(\mathbf{r})\left[\tfrac{1}{2} + 2\mathbf{S}_1 \cdot \mathbf{S}_2\right]. \tag{2.5}$$

(We neglect the smaller nuclear Zeeman terms and also all anisotropic terms as the radicals are assumed to be freely rotating in the solvent.) The first and second terms in (2.5) describe the hyperfine interaction acting between the unpaired electron spins $\mathbf{S}_1$, $\mathbf{S}_2$ and the nuclear spins $\mathbf{I}_k$, $\mathbf{I}_l$. The third (electron Zeeman) term describes the interaction between the electron spins and the applied magnetic field. The fourth term represents the exchange interaction of the unpaired electrons. As $J(\mathbf{r})$ rapidly decreases with the pair separation distance $\mathbf{r}$ one can safely neglect J over most of the diffusion path except in the contact region of the radicals.

At small pair separation the exchange interaction $J(\mathbf{r})$ splits the singlet and triplet radical pair states and for

$$J \gg \frac{e\hbar}{2mc}\left\{\sum_k |a_{1k}| + \sum_l |a_{2l}|\right\} \sim 10^{-6}\ \text{eV}$$

suppresses the hyperfine induced spin transitions and any magnetic field effect. The observation of a magnetic field modulation of the geminate recombination process gives, however, ample evidence that the recombining radicals must have been separated by a distance r at which $J(\mathbf{r}) \ll 10^{-6}$ eV for a time of at least a few nanoseconds, i.e., long enough for the hyperfine coupling to induce the singlet–triplet transition.

In the contact region, J is essential only for the generation of electron spin polarization of the separated radicals. It exerts, however, only a minor influence on the recombination yield and will be neglected in our further discussion.

For a system of M nuclear spins $\frac{1}{2}$ there are 2^{M+2} spin states to be considered for a representation of the electron–nuclear spin motion. This amounts to over four million states for the system $^2\text{Py}^{\cdot-} + {}^2\text{DMDMA}^{\cdot+}$ of Ref. 1. For the purpose of this study, which is mainly concerned with the diffusion process of radical pairs, such a detailed description is not necessary. We will instead consider a model system with one nuclear spin on each radical.

The third rhs term of Eq. (2.1) describes the occurrence of geminate recombination. The Feshbach optical potential $U(\mathbf{r})$, first introduced by Tomkiewicz *et al.*,[8] accounts for the extinction of radical pairs at distance $\mathbf{r}$ due to electron transfer. The optical potential $U(\mathbf{r})$ is strongly peaked around a distance r_1 at which the electron jump is most likely. We assume that r_1 is also the distance at which the radical pairs have been generated originally by electron transfer. In the coupled electron spin representation we take $U(\mathbf{r})$ to be diagonal, i.e., $U(\mathbf{r})$ only depletes singlet and triplet pairs but does not create or destroy electron spin phase,

$$U(\mathbf{r}) = s(\mathbf{r})[\kappa_S Q_S + \kappa_T Q_T]. \tag{2.6}$$

$s(\mathbf{r})$ is a measure of the probability for the recombination reaction to take place at distance $\mathbf{r}$, and the operators

$$Q_T = \tfrac{3}{4} + \mathbf{S}_1 \cdot \mathbf{S}_2, \qquad Q_S = 1 - Q_T, \tag{2.7}$$

project on the manifold of triplet and singlet states, respectively. Equation (2.6) implies that singlet [triplet] radical pairs in the reaction domain described by $s(\mathbf{r})$ undergo a first-order recombination process with rate constants $\kappa_S s(\mathbf{r})$ [$\kappa_T s(\mathbf{r})$]. To employ $U(\mathbf{r})$ in the form of (2.6) the rate constants have to be known. In Sec. III we will derive for the case of spin-independent recombination ($\kappa_S = \kappa_T$) the relationship between $\kappa_S(\kappa_T)$ and the second-order recombination rates $k_S(k_T)$ which are amenable to experimental measurement.

The geminate recombination rate of singlet [triplet] pairs $\dot{n}_S(t)$ [$\dot{n}_T(t)$] induced by the optical potential $U(\mathbf{r})$ is

$$\dot{n}_S(t) = -\int d\mathbf{r}\, tr\{Q_S[U(\mathbf{r})\rho(\mathbf{r},t) + \rho(\mathbf{r},t)U(\mathbf{r})]Q_S\},$$
$$\dot{n}_T(t) = -\int d\mathbf{r}\, tr\{Q_T[U(\mathbf{r})\rho(\mathbf{r},t) + \rho(\mathbf{r},t)U(\mathbf{r})]Q_T\}. \tag{2.8}$$

Substituting in the optical potential (2.6) yields the expression

$$\dot{n}_S(t) = -2\kappa_S \int d\mathbf{r}\, s(\mathbf{r})\, tr[Q_S\rho(\mathbf{r},t)Q_S],$$
$$\dot{n}_T(t) = -2\kappa_T \int d\mathbf{r}\, s(\mathbf{r})\, tr[Q_T\rho(\mathbf{r},t)Q_T]. \tag{2.9}$$

If the reaction domain $s(\mathbf{r})$ is spherically symmetric and closely centered around r_1, i.e., $s(\mathbf{r}) = \delta(r - r_1)/2$, then

$$\dot{n}_S(t) = -4\pi r_1^2 \kappa_S\, tr[Q_S\rho(r_1,t)Q_S],$$
$$\dot{n}_T(t) = -4\pi r_1^2 \kappa_T\, tr[Q_T\rho(r_1,t)Q_T], \tag{2.10}$$

assuming also spherical symmetry for $\rho(\mathbf{r},t)$. These equations illustrate an essential point of our study: a time-resolved observation of geminate recombination rates $\dot{n}_S(t)$ and $\dot{n}_T(t)$ provides a measure for $\mathrm{tr}\rho(r_1, t)$ which is just the time-dependent pair correlation of the reacting radicals, i.e., the probability for a radical pair initially at distance r_1 to be found still after time t at the same distance.

The last term of Eq. (2.1) describes the homogeneous recombination between radicals of different initial pairs where k is the second-order homogeneous recombination rate constant. This term can be eliminated from Eq. (2.1) by setting

$$\rho(\mathbf{r}, t) = c(t)\, P(\mathbf{r}, t). \tag{2.11}$$

$P(\mathbf{r}, t)$ describes the time evolution of an *isolated* radical pair and the scalar function $c(t)$ the depletion of radicals through homogeneous (interpair) recombination:

$$\frac{\partial}{\partial t} P(\mathbf{r}, t) = l(\mathbf{r})\, P(\mathbf{r}, t) - \frac{i}{\hbar}\,[H, P(\mathbf{r}, t)]^- - U(\mathbf{r})\, P(\mathbf{r}, t) - P(\mathbf{r}, t)\, U(\mathbf{r}), \tag{2.12}$$

$$\frac{d}{dt} c(t) = -k\,\langle p(t)\rangle\, c^2(t), \tag{2.13}$$

where $\langle p(t)\rangle = \int d\mathbf{r}\, \mathrm{tr} P(\mathbf{r}, t)$.

Once $P(\mathbf{r}, t)$ has been determined from Eq. (2.12), $c(t)$ can be evaluated readily:

$$c(t) = \frac{c_0}{1 + kc_0 \int_0^t d\tau \langle p(\tau)\rangle}. \tag{2.14}$$

For the experiments described in Ref. 1 the initial pair concentration c_0 was chosen small ($kc_0 \sim 10^{-4}\,\mathrm{ns}^{-1}$) and, hence, the homogeneous recombination was negligible over the time range 1–100 ns of geminate recombination. It should be pointed out that our treatment of the homogeneous recombination process is valid only in the limit of low pair concentration. The effect of the competition of 1, 2, 3, ... radicals for one reaction partner has been described recently for a stationary situation by Deutch *et al.*[14]

To account for the electron–nuclear spin motion of a radical pair one may employ the Heisenberg representation

$$P(\mathbf{r}, t) = \exp\left[-(i/\hbar) Ht\right] Y(\mathbf{r}, t) \exp\left[(i/\hbar) Ht\right], \tag{2.15}$$

which leaves one to solve

$$\frac{\partial}{\partial t} Y(\mathbf{r}, t) = l(\mathbf{r})\, Y(\mathbf{r}, t) - K(\mathbf{r}, t)\, Y(\mathbf{r}, t) - Y(\mathbf{r}, t) K(\mathbf{r}, t), \tag{2.16}$$

where

$$K(\mathbf{r}, t) = \exp\left[(i/\hbar) Ht\right] U(\mathbf{r}) \exp\left[-(i/\hbar) Ht\right]. \tag{2.17}$$

$Y(\mathbf{r}, t)$ obeys a diffusion equation with the time-dependent sink $K(\mathbf{r}, t)$ which accounts for the geminate recombination process. The time dependence of the recombination operator $K(\mathbf{r}, t)$ has an obvious interpretation: Due to the hyperfine interaction the electron spin state population varies in time which in turn induces a time-varying recombination rate.

In the case that the recombination process described by $U(\mathbf{r})$ is spin-dependent Eq. (2.16) constitutes a rather formidable set of coupled equations. A simple approximate solution can, however, be set up from Eq. (2.12) by the following argument: The electron–nuclear spin Hamiltonian commutes with the scalar operator $l(\mathbf{r})$ and with $U(\mathbf{r})$ except in the reaction domain $s(\mathbf{r})$. The spin-motion of radical pairs in this domain is governed by the complex Hamiltonian

$$H_U = H + i\,(\kappa_S Q_S + \kappa_T Q_T)\, s(\mathbf{r}). \tag{2.18}$$

Besides depleting the radical pairs the effect of the optical potential is to dampen the transition probability between singlet and triplet electron spin states. This has been illustrated in Ref. 1. If we neglect the latter effect, i.e., assume that H and U commute for all $\mathbf{r}$, $P(\mathbf{r}, t)$ takes the form

$$P(\mathbf{r}, t) \sim P_0(t)\, \mathrm{tr} P(\mathbf{r}, t), \tag{2.19}$$

where $P_0(t)$ is the electron–nuclear spin density matrix in a reaction-free system:

$$\frac{d}{dt} P_0(t) = -\frac{i}{\hbar}\,[H, P_0(t)], \tag{2.20}$$

We insert, however, this approximate expression for $P(\mathbf{r}, t)$ only into the second term of Eq. (2.12) which describes the electron–nuclear spin motion, i.e., we replace $-(i/\hbar)[H, P(\mathbf{r}, t)]$ by the expression

$$-(i/\hbar)[H, P_0(t)]\, \mathrm{tr} P(\mathbf{r}, t) = \dot{P}_0(t)\, \mathrm{tr} P(\mathbf{r}, t). \tag{2.21}$$

If one then averages the Liouville equation (2.12) over all nuclear spin states, i.e., assumes that all nuclear spin states exhibit identical singlet–triplet transition rates $\mathrm{tr}[Q_{S,T} \dot{P}_0 Q_{S,T}]$, a pair of coupled diffusion equations for the probabilities of singlet and triplet radical pairs defined by

$$p_S(\mathbf{r}, t) = \mathrm{tr}\left[Q_S P(\mathbf{r}, t)\, Q_S\right], \tag{2.22}$$

$$p_T(\mathbf{r}, t) = \mathrm{tr}\left[Q_T P(\mathbf{r}, t)\, Q_T\right] \tag{2.23}$$

can be derived

$$\frac{\partial}{\partial t} p_S(\mathbf{r}, t) = l(\mathbf{r})\, p_S(\mathbf{r}, t) + [p_S(\mathbf{r}, t) + p_T(\mathbf{r}, t)] \times \mathrm{tr}\left[Q_S \dot{P}_0(t)\, Q_S\right] - 2\kappa_S s(\mathbf{r})\, p_S(\mathbf{r}, t), \tag{2.24}$$

$$\frac{\partial}{\partial t} p_T(\mathbf{r}, t) = l(\mathbf{r})\, p_T(\mathbf{r}, t) + [p_S(\mathbf{r}, t) + p_T(\mathbf{r}, t)] \times \mathrm{tr}\left[Q_T \dot{P}_0(t)\, Q_T\right] - 2\kappa_T s(\mathbf{r})\, p_T(\mathbf{r}, t). \tag{2.25}$$

In a forthcoming publication[15] the spin-dependent geminate recombination of realistic radical ion pair systems will be studied along the lines of Eqs. (2.24) and (2.25). There the validity of the approximations leading to these equations will be demonstrated.

A spin-independent recombination process described by

$$U(\mathbf{r}) = \kappa s(\mathbf{r}) \tag{2.26}$$

renders the recombination operator (2.17) time-independent, namely, $K(\mathbf{r}, t) = U(\mathbf{r})$. In this case the diffusion equation is diagonal in the electron–nuclear spin states and can be solved readily. For reactions starting ini-

tially from a singlet radical pair at distance r_1, i.e.,

$$\rho(\mathbf{r}, 0) = c_0 \frac{\delta(r - r_1)}{4\pi r_1^2} \frac{Q_S}{Z_S} \tag{2.27}$$

(Z_S is the number of singlet electron-nuclear spin states), the density matrix takes on the simple form

$$\rho(\mathbf{r}, t) = c(t)\, p(\mathbf{r}, t) \exp[-(i/\hbar)Ht](Q_S/Z_S) \exp[(i/\hbar)Ht]. \tag{2.28}$$

where $p(\mathbf{r}, t)\, Q_S/Z_S$ is the diffusion distribution solving Eq. (2.16) subject to the initial condition

$$p(\mathbf{r}, 0) = \delta(r - r_1)/4\pi r_1^2 . \tag{2.29}$$

The rate of geminate triplet recombination products is then according to Eq. (2.10), with $s(\mathbf{r}) = \delta(r - r_1)/2$ and a spherically symmetric potential $V(\mathbf{r})$,

$$\dot{n}_T(t) = -4\pi r_1^2 \kappa_T c(t)\, tr\{Q_T \exp[-(i/\hbar)Ht] \times (Q_S/Z_S) \exp[(i/\hbar)Ht]\, Q_T\}\, p(r_1, t). \tag{2.30}$$

This expression illustrates that a measurement of the geminate triplet recombination rate $\dot{n}_T(t)$ yields directly the pair correlation function $p(r_1, t)$ describing the short time diffusion of radicals in the liquid. It is this special case of spin-independent recombination processes that we want to study in this paper. Furthermore, we shall assume as in Eq. (2.30) that the radical pair generation, diffusion, and recombination are independent of the relative orientation of the radicals and consider only spherically symmetric solutions to the stochastic Liouville equation (2.1).

III. GEMINATE AND HOMOGENEOUS RECOMBINATION DESCRIBED BY THE OPTICAL POTENTIAL $U(r)$

The radical recombination process as described by the Liouville Eq. (2.1) occurs in two steps: first, the diffusive separation and collision of the radicals $^2A^{\cdot}$ and $^2D^{\cdot}$ accounted for by the diffusion operator $l(r)$; and second, the electron jump and formation of singlet or triplet products accounted for by the optical potential $U(r)$:

$$^2A^{\cdot} + {}^2D^{\cdot} \xrightarrow[\text{separation + collision}]{l(r)} {}^{1,3}(^2A^{\cdot} + {}^2D^{\cdot}) \xrightarrow[\text{electron jump}]{U(r)} {}^{1,3}A + {}^1D.$$

Taking the concentration of radical pairs to be small enough in order to neglect the homogeneous recombination term in (2.1), we describe the recombination process by the diffusion equation

$$\frac{\partial}{\partial t} p(\mathbf{r}, t) = \{D\nabla \cdot [\nabla - \beta \mathbf{F}(\mathbf{r})] - 2s(\mathbf{r})\kappa_{S,T}\}\, p(\mathbf{r}, t). \tag{3.1}$$

The following treatment is exact only in the case of spin-independent recombination, i.e., $\kappa_S = \kappa_T = \kappa$. A treatment at high concentrations which includes the competition of several radicals for a reaction partner can be found in Ref. 14.

The rate at which radical pairs recombine

$$\dot{n}(t) = \frac{d}{dt} \int d\mathbf{r} p(\mathbf{r}, t) \tag{3.2}$$

can be determined from Eq. (3.1). If one assumes that the pair potential is spherically symmetric, then for the diffusion process with a minimal encounter distance r_1

$$\dot{n}(t) = 4\pi r_1^2 j(r_1, t) + 4\pi J_\infty - 2\kappa \int d\mathbf{r}\, s(\mathbf{r})\, p(\mathbf{r}, t), \tag{3.3}$$

where $j(r, t)$ is the radial flux density defined to be

$$j(r, t) = -D\left(\frac{\partial}{\partial r} - \beta F(r)\right) p(r, t). \tag{3.4}$$

If the recombination rate $\dot{n}(t)$ is considered to be solely due to the optical potential $s(\mathbf{r})\kappa$, then the flux of radicals at r_1, the first term in (3.3), must vanish, and one has to impose the boundary condition on the solution of (3.1)

$$j(r_1, t) = 0. \tag{3.5}$$

The term $4\pi J_\infty$ represents the flux condition at large separations ($r \to \infty$), and for an isolated system $J_\infty = 0$. We assume the optical potential is also spherically symmetric and peaked around r_1 and set

$$s(r) = \delta(r - r_1)/2, \tag{3.6}$$

in which case the recombination rate (3.3) becomes

$$\dot{n}(t) = 4\pi r_1^2 [J_\infty / r_1^2 - \kappa p(r_1, t)]. \tag{3.7}$$

As geminate and homogeneous recombination processes are due to the same reaction events (diffusive encounters and electron back transfer), Eq. (3.1) serves to describe both. If we now assume Eqs. (3.1) and (3.7) describe the homogeneous recombination, we can use the stationary solution ($\partial p/\partial t = 0$, $J_\infty \neq 0$) to relate the rate constant κ to the macroscopic second-order recombination rate constant k defined by

$$\dot{N} = k[^2A^{\cdot}][^2D^{\cdot}]. \tag{3.8}$$

This requires that the stationary solution of Eq. (3.1) satisfies the additional boundary condition

$$p(r) \underset{r \to \infty}{\sim} [^2A^{\cdot}][^2D^{\cdot}] \exp[-\beta V(r)], \tag{3.9}$$

i.e., the correlation function $p(r)$ goes asymptotically to the Boltzmann distribution. Our treatment will be similar to that of Debye[16] and Eigen[17] except that we incorporate a reduced reaction probability of the encounter complex $^{1,3}(^2A^{\cdot} + {}^2D^{\cdot})$ due to the finite rate constant κ.

Under stationary conditions, it follows from Eq. (3.1) that the radial flux $r^2 j(r)$ which can also be written

$$r^2 j(r) = -r^2 D\, e^{-\beta V(r)} \frac{\partial}{\partial r} p(r)\, e^{\beta V(r)} \tag{3.10}$$

must be a constant, $-J_1$, say. J_1 can be evaluated from Eq. (3.7) for the condition $\dot{n}(t) = 0$, i.e., $J_1 = J_\infty = r_1^2 \kappa p(r_1)$, and upon integrating (3.10) one obtains

$$p(r) = [^2A^{\cdot}][^2D^{\cdot}] e^{-\beta V(r)} - \frac{\kappa r_1^2 p(r_1)}{D e^{\beta V(r)}} \int_r^\infty dR\, R^{-2}\, e^{\beta V(R)}. \tag{3.11}$$

Since the rate at which the recombination products are

formed is $\dot{N} = 4\pi r_1^2 \kappa p(r_1)$, the second-order rate constant k as defined in (3.8) can be determined (in units of $cm^3\ s^{-1}$)

$$k = \frac{4\pi D / \int_{r_1}^{\infty} dR\, R^{-2} \exp[\beta V(R)]}{1 + D\exp[\beta V(r_1)]/r_1^2 \kappa \int_{r_1}^{\infty} dR\, R^{-2} \exp[\beta V(R)]}. \quad (3.12)$$

This expression is identical to the Debye-type correction formula found in the treatments of diffusion effects on reaction rate constants when the reaction volume is taken to be the annular volume of the contact region.[18] The limit of diffusion-controlled recombination in which the ions react upon every encounter is attained for large rate constants κ:

$$\lim_{\kappa \to \infty} k = 4\pi D \Big/ \int_{r_1}^{\infty} dR\, R^{-2} \exp[\beta V(R)]. \quad (3.13)$$

Clearly, the effect of a finite κ is to reduce the second-order recombination rate constant below the diffusion-controlled value.

For recombination processes of neutral radicals and radical ions, simple analytical expressions for the second-order rate constants can be derived. In the case of free diffusion [$V(r) = 0$]

$$k = 4\pi D r_1 / (1 + D/\kappa r_1) \quad (3.14)$$

and in the case of oppositely charged radical ions [$V(r) = -e^2/\epsilon r$]

$$k = \frac{4\pi D r_L \Big/ \left[1 - \exp\left(\frac{-r_L}{r_1}\right)\right]}{1 + D\exp\left(\frac{-r_L}{r_1}\right) r_L \Big/ r_1^2 \kappa \left[1 - \exp\left(\frac{-r_L}{r_1}\right)\right]}, \quad (3.15)$$

where $r_L = \beta e^2/\epsilon$ is the so-called Onsager radius, i.e., the distance at which the separate ions assume an energy $-kT$. Equations (3.14) and (3.15) establish the desired connection between the microscopic optical potential $U(r) = \kappa \frac{1}{2} \delta(r - r_1)$ and the macroscopic second-order rate constant k. A general expression for the bimolecular reaction rate constant when the optical potential extends over a finite region is found in Ref. 7(c).

The notion of the dielectric screening of the Coulomb force described by the macroscopic dielectric constant ϵ cannot be expected to hold over microscopic distances of a few molecular diameters. Hermanson[19] has described for a Hartree–Fock potential of a bare electron–hole pair in a rare gas solid the dielectric screening by the random phase approximation and obtained the modified Coulomb potential

$$V(r) = -\frac{e^2}{\epsilon r}\left[1 + (\epsilon - 1)\exp\left(\frac{-r}{b}\right)\right]. \quad (3.16)$$

The "breakdown length" b, related to crystal properties, was found to be smaller than an atomic diameter and of order 1 Å. We will assume that the diffusion of ions over microscopic distances can be described by this static potential of a rare gas solid environment in order to see what effect a dielectric "descreening" (i.e., a factual reduction of the dielectric constant at short distances) may have on the recombination of radical ions.

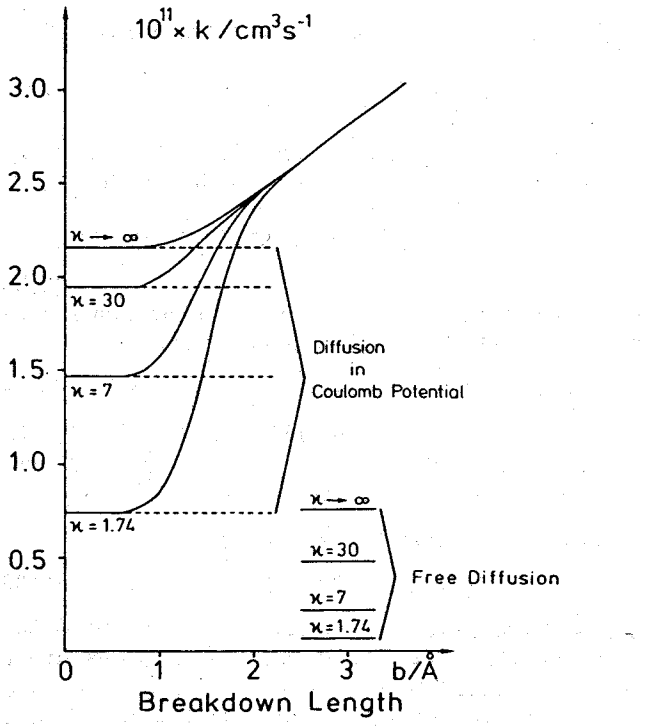

FIG. 1. Dependence of the second-order recombination rate constant k on the breakdown length in solvents with the microscopic dielectric screening described by the Hermanson potential (3.16) with $\epsilon = 35$ for the optical potential strengths $\kappa = 1.74$ Å ns^{-1}, 7 Å ns^{-1}, 30 Å ns^{-1}, ∞. Also presented are the recombination rate constants for free diffusion and for diffusion in a Coulomb potential with $\epsilon = 35$ (at $T = 298$ K, $D = 10^{-5}\ cm^2\ s^{-1}$).

In Fig. 1 we compare the second-order recombination rate constants k for freely diffusing radicals, for radical ions diffusing in an attractive Coulomb potential (with $\epsilon = 35$), and for radicals diffusing in the Hermanson potential (3.16) for various breakdown lengths. Smallest in value are the rate constants for free diffusion evaluated from Eq. (3.14). Figure 1 demonstrates that the second-order rate constants for free diffusion and recombining ions as evaluated from (3.15) are lowered from the diffusion-controlled values ($\kappa \to \infty$) as κ decreases. The rate constants evaluated using the Hermanson potential coincide with the rate constants for the Coulomb potential at small breakdown lengths as (3.16) goes to the Coulomb potential for $b = 0$. However, as b increases the second-order rate constants become greater than the Debye diffusion-controlled value ($\kappa \to \infty$) and eventually coalesce.

IV. RECOMBINATION OF RADICAL PAIRS UNDERGOING FREE BROWNIAN MOTION

In this section we consider the geminate recombination of a radical pair undergoing free Brownian motion for which case analytical expressions for the recombination rate $\dot{n}(t)$ and the triplet quantum yield $\phi_T(t, B)$ can be obtained. Though somewhat unrealistic, the free Brownian motion description of radical recombination is most attractive in that it allows a simple analytical formulation which bears all the essential features of the more general situation. For radical pairs moving

in a force field only a numerical description is possible which will be furnished in Sec. V.

In view of the experimental observations of Ref. 1, the quantity of chief interest is the rate of geminate triplet recombination $\dot{n}_T(t)$ defined by Eq. (2.8). Assuming the radical pair concentration to be low enough to neglect the homogeneous, second-order recombination during the geminate phase, we set $c(t) = c_0 = 1$. Furthermore, we consider the recombination to be spin-independent, i.e. $\kappa_T = \kappa_S = \kappa$ in (2.6). This yields according to Eq. (2.30)

$$\dot{n}_T = -4\pi r_1^2 \kappa W_T(t, B) p(r_1, t), \tag{4.1}$$

where we have defined

$$W_T(t, B) = tr\left[Q_T \exp\left(-\frac{i}{\hbar} Ht\right)\left(\frac{Q_S}{Z_S}\right) \exp\left(\frac{i}{\hbar} Ht\right) Q_T\right].$$

In Sec. III the connection between κ and the second-order rate constant k of homogeneous recombination has been established

$$k = (\kappa/\alpha)\, 4\pi D r_1, \tag{4.2}$$

where

$$\alpha = \kappa + D/r_1.$$

In this expression the factor $4\pi D r_1$ is the diffusion-controlled rate for a radical pair encounter (approach of two radicals to the distance r_1) and the factor κ/α is the probability for the pair to react after the encounter.

The function $W_T(t, B)$ gives the probability for a radical pair initially ($t = 0$) in a singlet electron spin state to be found at time t in a triplet spin state. For a system of two radicals each with a half-spin nucleus and electron–nuclear spin coupling constant a, the following expression can be derived (see for example Ref. 6):

$$\begin{aligned} W_T(t, B) = {} & \tfrac{1}{2} S_1(\omega_1, t) - \tfrac{1}{4}\left[S_1(\omega_1, t) - 3S_1(\omega_2, t)\right. \\ & \left. - \tfrac{1}{2} S_1(\omega_1 + \omega_2, t) - \tfrac{1}{2} S_1(\omega_1 - \omega_2, t)\right](\omega_1/\omega_2)^2 \\ & - \tfrac{1}{4}\left[S_1(\omega_2, t) - \tfrac{1}{4} S_1(2\omega_2, t)\right](\omega_1/\omega_2)^4, \end{aligned} \tag{4.3}$$

where

$$\omega_1 = \tfrac{1}{2}(ge/2mc)\, a, \quad \omega_2 = \omega_1\left[1 + (B/a)^2\right]^{1/2},$$

and

$$S_1(\omega, t) = \sin^2 \omega t\,. \tag{4.4}$$

The magnetic field B and the coupling constant a are both in units of Gauss. At high magnetic fields,[2] i.e., $\omega_1/\omega_2 \to 0$, this expression simplifies to $W_T(t) = \frac{1}{2}\sin^2\omega_1 t$, and at low magnetic fields,[20] i.e., $\omega_1/\omega_2 \to 1$, to $W_T(t) = \frac{3}{4}\sin^2\omega_1 t + \frac{3}{16}\sin^2 2\omega_1 t$. Figure 2 illustrates the time and magnetic field dependence of $W_T(t, B)$ assuming $a = 50$ G. This value of the coupling constant is roughly equal to the sum of the coupling constants in each of the radicals $^2Py^{\cdot}$ ($\sum_k a_{1k} \simeq 30$ G) and ^{2}DMDMA$^{\cdot}$ ($\sum_l a_{2l} \simeq 56$ G) in Ref. 1. The combination of the hyperfine coupling constants on each radical into a single coupling constant accelerates the initial buildup of $W_T(t, B)$ and produces oscillations at longer times which are damped in most realistic spin systems.[1,15]

The radical pairs described by Fig. 2 are initially all in the singlet state, i.e., $W_T(0, B) = 0$. As time evolves the pairs oscillate between the singlet and the triplet state. In the field free case, $B = 0$ G, the radical pairs reach a maximum triplet probability of 75% at about 3.5, 10.5, 17.5, ... ns and a minimum triplet probability of zero at about 7, 14, 21, ... ns. For magnetic fields above 120 G only a 50% triplet probability is reached at times 4, 12, 18, ... ns. The modulation of the spin motion at intermediate fields is lucidly demonstrated by the wave pattern in Fig. 2.

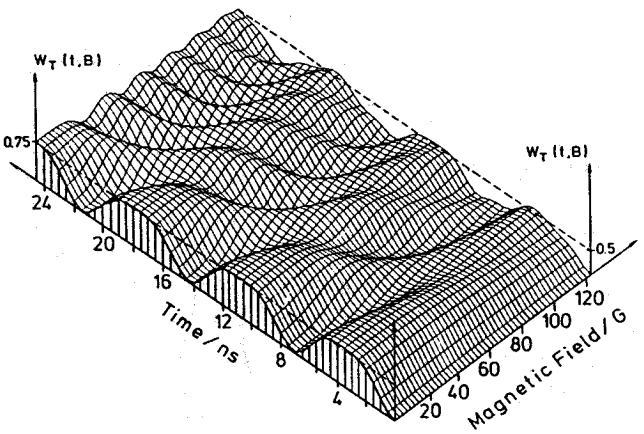

FIG. 2. Time and magnetic field dependence of the hyperfine induced singlet–triplet transition probability as given by Eq. (4.3) with $a = 50$ G. The pairs are initially all in the singlet state, i.e., $W_T(0, B) = 0$.

The pair correlation function $p(r_1, t)$ is related, of course, to the distribution function $p(r, t)$ of the radical pair. If one assumes free Brownian motion, the distribution function is the solution of the diffusion equation with a sink

$$\frac{\partial}{\partial t} p(\mathbf{r}, t) = D\nabla^2 p(\mathbf{r}, t) - \kappa\delta(r - r_1)\, p(\mathbf{r}, t). \tag{4.5}$$

This equation is equivalent to the elementary diffusion equation

$$\frac{\partial}{\partial t} p(\mathbf{r}, t) = D\nabla^2 p(\mathbf{r}, t) \tag{4.6}$$

subject to the radiation boundary condition (assuming spherical symmetry)[21]

$$\frac{\partial}{\partial r} p(r, t) = \frac{\kappa}{D} p(r, t) \quad \text{at} \quad r = r_1. \tag{4.7}$$

We assume for the distribution function the initial condition

$$p(r, 0) = \delta(r - r_1)/4\pi r_1^2, \tag{4.8}$$

which implies that the radical pairs are generated through electron transfer $^1\overset{*}{A} + {}^1D \to {}^2A^{\cdot} + {}^2D^{\cdot}$ all at distance r_1, the same distance at which recombination, i.e., electron back transfer $^2A^{\cdot} + {}^2D^{\cdot} \to {}^{1,3}A + {}^1D$, takes place. The solution to Eqs. (4.6)–(4.8) has been given by Carslaw and Jaeger.[22] It can be written in the simple form

$$\begin{aligned} p(r, t) = {} & \frac{\exp\left[-(r - r_1)^2/4Dt\right]}{4\pi r r_1 \sqrt{4\pi D t}} \\ & \times\left(2 - \frac{F\left[\alpha\sqrt{t/D} + (r - r_1)/\sqrt{4Dt}\right]}{\frac{1}{2} + (r - r_1)/4\alpha t}\right), \end{aligned} \tag{4.9}$$

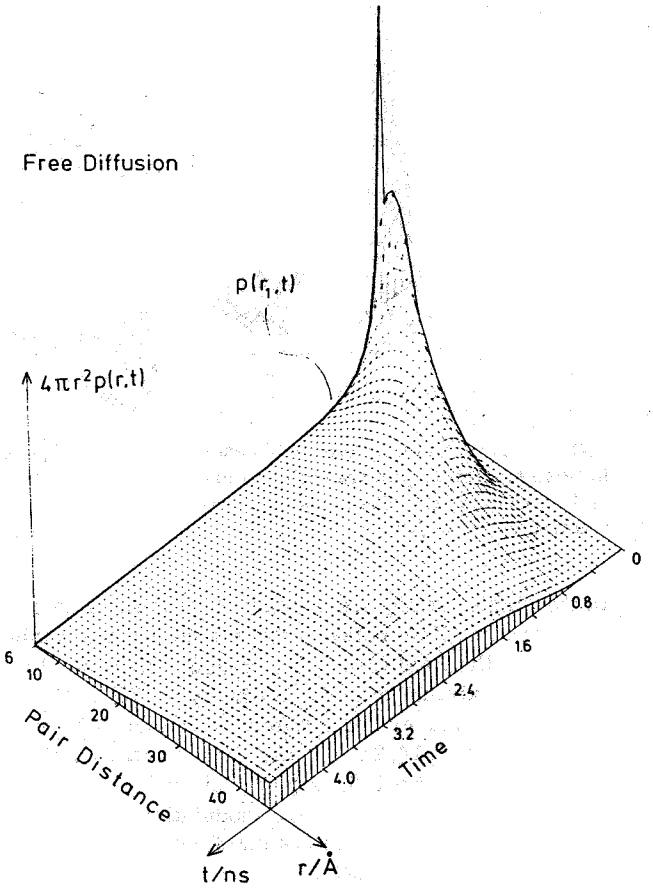

FIG. 3. Space- and time-dependent pair distribution $4\pi r^2 p(r,t)$ of Eq. (4.9) for radicals undergoing free Brownian motion. The radical pairs are generated initially at $r_1 = 6$ Å and also recombine at r_1 with a total recombination yield $\kappa/\alpha = 0.1$. The initial distribution is reduced in height to fit the illustration. The correlation function $p(r_1, t)$ at the inner boundary is related according to Eq. (4.1) to the recombination rate $n_T(t)$.

where

$$F(z) = \sqrt{\pi}\, z \exp(z^2)\,\mathrm{erfc}(z), \tag{4.10}$$

erfc(z) standing for the complementary error function

$$\frac{2}{\sqrt{\pi}} \int_z^\infty e^{-t^2}\, dt.$$

For an evaluation of (4.10) the following expressions proved well convergent[23]

$$F(z) = \cfrac{1}{1 + \cfrac{1/2z^2}{1 + \cfrac{1/z^2}{1 + \cfrac{3/2z^2}{1 + \ldots}}}}, \qquad 1.5 < |z| < \infty, \tag{4.11}$$

$$F(z) = \sqrt{\pi}\, z \exp(z^2)\left(1 - \frac{1}{\sqrt{\pi}} \sum_{n=0}^{\infty} (-1)^n z^{2n+1}/n!\,(n+\tfrac{1}{2})\right), \qquad 0 \le |z| \le 1.5 \tag{4.12}$$

The radical pair distribution function $4\pi r^2 p(r,t)$ is presented in Fig. 3 both as a function of the pair distance r and time t. In evaluating the distribution we have assumed $\kappa/\alpha = 0.1$, i.e., 10% of the radical pairs recombine, the remainder separate completely, and that the radical pairs are initially generated at a distance $r_1 = 6$ Å. At $t = 4$ ns the bulk of the pairs have diffused more than 20 Å apart and only very few are still in contact. The number of radical pairs in contact, given by the pair correlation function $p(r_1, t)$, decreases rapidly in time as illustrated by Fig. 3. So does the total recombination rate $\dot{n}(t) = -4\pi r_1^2 \kappa p(r_1, t)$:

$$\dot{n}(t) = -\frac{\kappa}{\sqrt{\pi D t}} \left[1 - F(\alpha\sqrt{t/D})\right]. \tag{4.13}$$

The rapid diffusive separation of the radical pairs and the concomitant decrease of the pair correlation function $p(r_1, t)$ counteracts the recombination to singlet and triplet products. The total recombination yield $\phi(t)$ provides, hence, a qualitative measure of the pair separation:

$$\phi(t) = -\int_0^t \dot{n}(\tau)\, d\tau = (\kappa/\alpha)\left[1 - e^{\alpha^2 t/D}\,\mathrm{erfc}(\alpha\sqrt{t/D})\right]. \tag{4.14}$$

As $\lim_{x\to\infty} e^{x^2}\,\mathrm{erfc}(x) = 0$, the total recombination yield is

$$\lim_{t\to\infty} \phi(t) = \kappa/\alpha, \tag{4.15}$$

as to be expected from the expression (4.2) for the second-order recombination rate constant.

However, only the yield $\phi_T(t, B)$ of triplet recombination products

$$\phi_T(t, B) = -\int_0^t W_T(\tau, B)\, \dot{n}(\tau)\, d\tau \tag{4.16}$$

is accessible to experimental observation as has been discussed in Ref. 1. In order to determine $\phi_T(t, B)$ it is necessary to evaluate the integral

$$S_2(\omega, t) = -\int_0^t S_1(\omega, \tau)\, \dot{n}(\tau)\, d\tau. \tag{4.17}$$

Replacing $S_1(\omega, t)$ in Eq. (4.3) by $S_2(\omega, t)$ yields $\phi_T(t, B)$. One obtains from (4.4) and (4.13)

$$S_2(\omega, t) = \frac{\kappa}{2\alpha}\left[\frac{1}{1+y^2} - \sqrt{2y}\,\frac{C(2\omega t) - yS(2\omega t)}{1+y^2} - e^{\alpha^2 t/D}\,\mathrm{erfc}(\alpha\sqrt{t/D})\left(1 - \frac{\cos 2\omega t + \frac{1}{y}\sin 2\omega t}{1+y^{-2}}\right)\right], \tag{4.18}$$

where $y = \alpha^2/2\omega D$ and $C(x)$ and $S(x)$ are the Fresnel integrals

$$C(x) = \sqrt{\frac{1}{2\pi}} \int_0^x \frac{\cos t}{\sqrt{t}}\, dt, \tag{4.19}$$

$$S(x) = \sqrt{\frac{1}{2\pi}} \int_0^x \frac{\sin t}{\sqrt{t}}\, dt, \tag{4.20}$$

which can be evaluated by virtue of

$$C(x) + iS(x) = \frac{1+i}{2}\left[1 - \mathrm{erfc}\left((1-i)\sqrt{\frac{x}{2}}\right)\right]. \tag{4.21}$$

For the evaluation of the complex error function erfc(z), the expressions (4.11) and (4.12), analytically continued

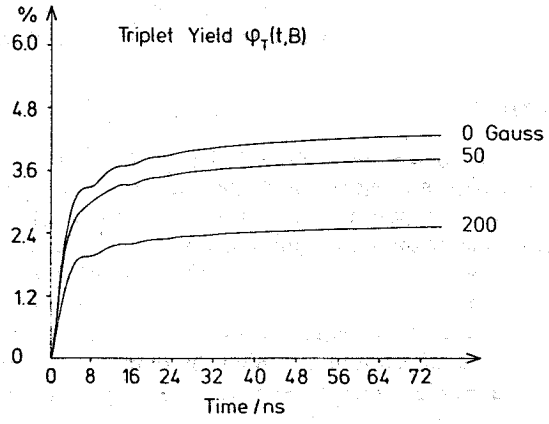

FIG. 4. Time-dependent yield of triplet recombination products $\phi_T(t,B)$ evaluated from Eqs. (4.3) and (4.18) for $D = 10^{-5}$ cm^2 s^{-1}, $\kappa/\alpha = 0.5$, $a = 50$ G and $B = 0$, 50, and 200 G.

to the complex plane, can be employed.

The time evolution of the triplet yield ϕ_T is presented in Fig. 4 for magnetic fields 0, 50, and 200 G assuming a diffusion constant $D = 10^{-5}$ cm^{2}s^{-1} and a total recombination yield $\kappa/\alpha = 0.5$. One observes that $\phi_T(t)$ rises rapidly within about 4 ns and then grows slowly to its asymptotic value $\phi_T(\infty, B)$. Some quantum beats due to the oscillations of the triplet probability $W_T(t, B)$ are clearly discernible. The total triplet yield $\phi_T(\infty, B)$ depends strongly on the applied magnetic field B. At 0 G the total yield is 4.8%, at 50 G it is 3.7%, and at 200 G it drops to 2.8%.

The total triplet yield can be evaluated by taking the limit $t \to \infty$ of $S_2(\omega, t)$ as given in Eq. (4.18). As $C(x)$ and $S(x)$ both go asymptotically to a value $\frac{1}{2}$ and $e^{x^2}\mathrm{erfc}(x)$ vanishes for large x, one obtains

$$S_3(\omega) = \lim_{t\to\infty} S_2(\omega, t) = \frac{\kappa/2\alpha}{1+y^2}\left(1 - \sqrt{\frac{y}{2}}\,(1-y)\right), \qquad (4.22)$$

where y is as defined in (4.18). Replacing $S_1(\omega, t)$ in Eq. (4.3) by $S_3(\omega)$ gives then the total triplet yield $\phi_T(\infty, B)$.

According to Eqs. (4.22) and (4.3) the yield of geminate triplet products $\phi_T(\infty, B)$ is controlled by the diffusion constant D, the strength of the hyperfine coupling a, the applied magnetic field B, and the recombination probability κ/α. The influence of these factors on $\phi_T(\infty, B)$ is demonstrated in Fig. 5. In Fig. 5(a) the total triplet yield $\phi_T(\infty, B)$ is plotted as a function of both the diffusion constant D and the magnetic field B. The triplet yield is shown to decrease with increasing diffusion constant. This result is to be expected as a faster diffusion of the radicals shortens the recombination time and, therefore, the probability for the radicals to be in a triplet state at the instance of the reaction is decreased. Figure 5(a) also reveals the peculiar magnetic field dependence of $\phi_T(\infty, B)$. The triplet yield first increases from its zero field value of 11% (for $D = 10^{-6}$ cm^{2}s^{-1}) to a maximum value of 12% at about 10 G and then decreases to a value of 7% at 200 G, corresponding to a relative magnetic field effect $\phi_T(\infty, 200\,\mathrm{G})/\phi_T(\infty, 0) = 0.58$. This qualitative behavior of the triplet

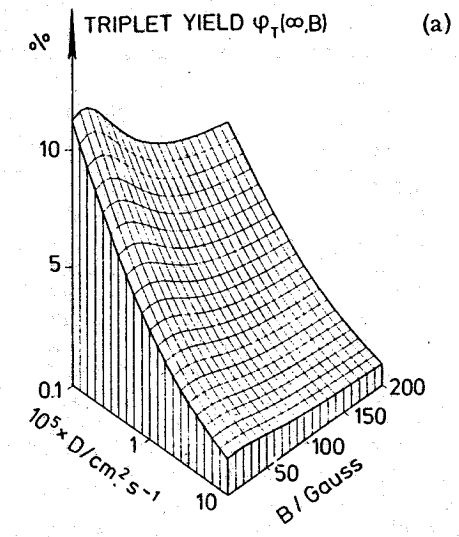

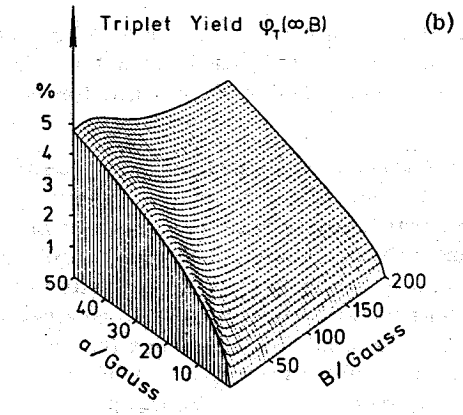

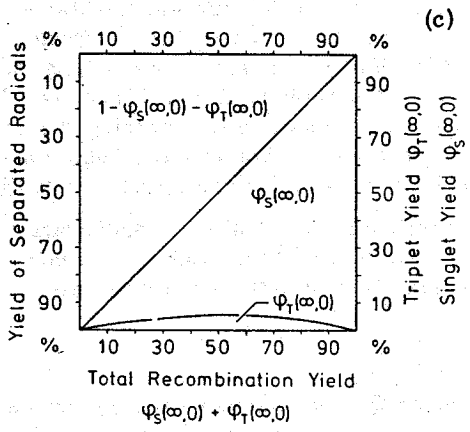

FIG. 5. Yield of triplet recombination products $\phi_T(\infty, B)$ evaluated from Eqs. (4.3) and (4.22) as (a) a function of the applied magnetic field B and the diffusion constant D for $\kappa/\alpha = 0.5$, $a = 50$ G; (b) a function of the applied magnetic field B and the hyperfine coupling constant a for $\kappa/\alpha = 0.5$, $D = 10^{-5}$ cm^2 s^{-1}. (c) Partition of the pair recombination into singlet and triplet products and separated radicals for $a = 50$ G, $D = 10^{-5}$ cm^2 s^{-1}, and $B = 0$.

yield is quite independent of D. The relative magnetic field effect varies only slightly with the diffusion constant.

Figure 5(b) exhibits the dependence of the triplet yield $\phi_T(\infty, B)$ on the hyperfine coupling constant a. The larger a, the faster is the hyperfine coupling induced singlet–triplet transition of the radical pair and the more likely are the radicals to recombine to triplet products before they separate. This expected behavior is reflected by the increase of $\phi_T(\infty, B)$ with increasing a. Most interesting is the effect of the hyperfine coupling strength on the magnetic field dependence of the triplet yield. For small a (e.g., $a = 10$ G) the triplet yield exhibits its main magnetic field dependence at low fields of about 10 G. For larger a (e.g., $a = 50$ G) stronger fields (50–100 G) are needed to reduce $\phi_T(\infty, B)$. The magnetic field dependence of $\phi_T(\infty, B)$ is, hence, a measure for the strength of hyperfine coupling in the recombining radicals. The relative magnetic field effect given by $\phi_T(\infty, 200\text{ G})/\phi_T(\infty, 0)$ varies only slightly with a, e.g., it is 0.58 for $a = 50$ G, 0.53 for $a = 25$ G, and 0.50 for $a = 10$ G (for $D = 10^{-5}$ cm^{2}s^{-1}).

Figure 5(c) shows how the geminate process partitions the initial radical pairs into singlet products, triplet products, and separate radicals ($D = 10^{-5}$cm^{2}s^{-1}, $a = 50$ G, $B = 0$). One observes that triplet product formation is at a maximum for a total recombination yield $\kappa/\alpha = \phi_S(\infty, 0) + \phi_T(\infty, 0)$ of 50%, in which case 45% of the pairs form singlet products, 5% triplet products, and 50% of the pairs separate. For a larger recombination probability, i.e., higher total recombination yields κ/α, the pairs recombine too fast for the hyperfine coupling to induce triplet products. For a total recombination yield κ/α of 90% one has 88% singlet products, only 2% triplet products, and 10% separated radicals. Of course, also for small recombination probabilities there is little triplet product formation, e.g., for $\kappa/\alpha = 0.1$ there are 8.5% singlet products, 1.5% triplet products, and 90% separated radicals.

The free Brownian motion model for the geminate recombination of radical pairs has also been employed by Evans *et al.*[6] for the case $\kappa_T = 0$ and a delta-function exchange interaction. These authors obtained an approximate expression for the *total* yield of singlet recombination products $\phi_S(\infty, B)$ in specific nuclear spin states which provides a measure for the NMR (CIDNP) spectra of the diamagnetic radical products.

We have demonstrated in this section by way of a simple analytical treatment the hyperfine-induced recombination of radical pairs undergoing free Brownian motion. The model of free Brownian motion is, of course, quite crude as it neglects the Coulomb attraction of the ionic radicals as well as force fields generated by the liquid molecules surrounding the radical pair.

V. RECOMBINATION OF RADICAL PAIRS UNDERGOING BROWNIAN MOTION IN A COULOMB POTENTIAL

We want to describe now the spin-independent ($\kappa_S = \kappa_T$) recombination of radical ions by the pair distribution function of two Brownian particles moving under the action of Coulomb attraction. For the radical ion pairs we assume again the initial condition (2.29) and take the diffusion and recombination processes to be spherically symmetric. The pair distribution function satisfies the Smoluchowski equation with a sink

$$\frac{\partial}{\partial t} p(r,t) = \left[D r^{-2} \frac{\partial}{\partial r} r^2 \left(\frac{\partial}{\partial r} + \beta \frac{\partial V(r)}{\partial r} \right) - u(r) \right] p(r,t)$$
$$= [l(r) - u(r)] p(r,t), \tag{5.1}$$

where $V(r) = -e^2/\epsilon r$ and ϵ is the macroscopic dielectric constant of the medium. A more realistic description of the dielectric screening of the Coulomb forces through the solvent medium over short distances by the Hermanson potential will also be discussed below.

It appears that an analytic solution exists only for the steady-state problem (Sec. III) and that the time-dependent problem must be solved numerically. Formally one can integrate the diffusion equation (5.1):

$$p(r,t) = \exp\{t[l(r) - u(r)]\} p(r,0). \tag{5.2}$$

If the spectrum and eigenfunctions of $l(r) - u(r)$ are known, one can expand the initial distribution $p(r, 0)$ in the eigenfunction basis and thereby evaluate $p(r, t)$. However, the eigenvalue problem cannot be solved analytically, and we pose instead an approximate formulation which can be solved numerically.

A. Differential-difference approximation to the Smoluchowski equation

To construct a finite-difference approximation for the spatial operator $l(r) - u(r)$ we follow a treatment similar to that of Pedersen and Freed.[7] The diffusion space $\{r, r_1 \le r < \infty\}$ is partitioned into a set of discrete spheres S_i or radius r_i and width h_i:

$$S_i = \{r, r_i \le r < r_i + h_i\}, \quad i = 1, 2, \ldots,$$

and the continuous distribution of radical pairs $p(r, t)$ is approximated by a discrete vector $\mathbf{P}(t)$:

$$\mathbf{P}(t) = \begin{bmatrix} P_1(t) \\ P_2(t) \\ \cdot \\ \cdot \\ P_N(t) \end{bmatrix}, \tag{5.3}$$

where $P_i(t)$ gives the concentration of radical pairs in S_i at time t. The finite-difference approximation assumes that the Brownian motion takes place by random jumps between adjacent spheres S_{i-1}, S_i, S_{i+1} and replaces the continuous diffusion operator $l(r)$ by a transition matrix L. The elements of L are obtained by approximating the differential operator $l(r)$ by the three-point difference formula[24]:

$$(L\mathbf{P})_j = \frac{2D}{r_j} \left(\frac{r_{j+1} P_{j+1}}{h_j (h_j + h_{j-1})} - \frac{r_j P_j}{h_j h_{j-1}} + \frac{r_{j-1} P_{j-1}}{h_{j-1} (h_j + h_{j-1})} \right)$$
$$+ \beta D \frac{\partial V(r_j)}{\partial r} \frac{P_{j+1} - P_{j-1}}{h_j + h_{j-1}} + \frac{\beta D}{r_j^2} v(r_j) P_j . \tag{5.4}$$

L becomes then a nonsymmetric, tridiagonal matrix

with elements $(2 \le j \le N-1;\ \bar{h}_j = (h_j + h_{j-1})/2;\ h_N \equiv h_{N-1})$

$$L_{jj} = \frac{-2D}{h_j h_{j-1}} + \frac{\beta D}{r_j^2} \upsilon(r_j),$$

$$L_{jj+1} = \frac{2Dr_{j+1}}{r_j h_j (h_j + h_{j-1})} + \frac{\beta D \frac{\partial V(r_j)}{\partial r}}{h_j + h_{j-1}},$$

$$L_{jj-1} = \frac{2Dr_{j-1}}{r_j h_{j-1}(h_j + h_{j-1})} - \frac{\beta D \frac{\partial V(r_j)}{\partial r}}{h_j + h_{j-1}},$$

$$L_{11} = -2 \frac{r_2^2 \bar{h}_2}{r_1^2 h_1} L_{21}, \tag{5.5}$$

$$L_{12} = -2 \frac{r_2^2 \bar{h}_2}{r_1^2 h_1} L_{22} - 2 \frac{r_3^2 \bar{h}_3}{r_1^2 h_1} L_{32}$$

$$L_{NN} = -2 \frac{r_{N-1}^2 \bar{h}_{N-1}}{r_N^2 h_N} L_{N-1N}$$

$$L_{NN-1} = -2 \frac{r_{N-1}^2 \bar{h}_{N-1}}{r_N^2 h_N} L_{N-1N-1} - 2 \frac{r_{N-2}^2 \bar{h}_{N-2}}{r_N^2 h_N} L_{N-2N-1}$$

where $\upsilon(r)$ is an approximation to the divergence term $(\partial/\partial r)\, r^2 (\partial V/\partial r)$:

$$\upsilon(r_j) = \frac{r_{j+1}^2 \frac{\partial V(r_{j+1})}{\partial r} - r_{j-1}^2 \frac{\partial V(r_{j-1})}{\partial r}}{h_j + h_{j-1}}. \tag{5.6}$$

We introduce also a further approximation and truncate the diffusion space at r_N such that the distribution vector $\mathbf{P}(t)$ and the diffusion operator L become finite.

The approximate problem to be solved is then posed by the differential–difference equation

$$\frac{d}{dt} \mathbf{P}(t) = [L - U] \mathbf{P}(t), \tag{5.7}$$

where the sink term $-U$ is connected with the optical potential $u(r) = 2\kappa s(r)$ by the approximation

$$U_{ii} = u(r_i). \tag{5.8}$$

Equation (5.7) has the formal solution

$$\mathbf{P}(t) = \exp\{t[L - U]\} \mathbf{P}(0), \tag{5.9}$$

which poses the eigenvalue problem

$$[L - U] \mathbf{Q}_i = \lambda_i \mathbf{Q}_i. \tag{5.10}$$

Once the eigenvalues λ_i and eigenvectors $\mathbf{Q}_i$ have been determined, the time evolution of the distribution can be evaluated readily by virtue of

$$\mathbf{P}(t) = \sum_i \mathbf{Q}_i \cdot \mathbf{P}(0)\, e^{t\lambda_i} \mathbf{Q}_i. \tag{5.11}$$

The number of radical pairs at time t evaluated according to the composite trapezoidal rule is

$$n(t) = \sum_i 4\pi r_i^2 h_i w_i P_i(t), \tag{5.12}$$

where the weights w_i are $w_1 = \frac{1}{2}$, $w_N = \frac{1}{2}$, $w_i = (1 + h_{i-1}/h_i)/2$ for $i = 2, 3, \ldots, N-1$. The recombination rate is by virtue of (5.7)

$$\dot{n}(t) = \sum_j \left(\sum_i 4\pi r_i^2 h_i w_i [L - U]_{ij} \right) P_j(t). \tag{5.13}$$

From the definition (5.5) of L it follows, however, that

$$\sum_i 4\pi r_i^2 h_i w_i L_{ij} = 0, \tag{5.14}$$

so that

$$\dot{n}(t) = -\sum_i 4\pi r_i^2 h_i w_i U_{ii} P_i. \tag{5.15}$$

The depletion of radical pairs is solely due to the optical potential U, the Brownian motion described by the transition operator L does not consume particles, as of course is to be expected. Condition (5.14) implies that the rows of L are linearly dependent, i.e., $\det L = 0$. It follows that the matrix L has at least one eigenvalue zero. Furthermore, one can show that L is negative semidefinite and, accordingly, as $u(r) > 0$ the operator $L - U$ is negative definite, i.e , has only negative eigenvalues.

The δ-function optical potential $\kappa\delta(r - r_1)$ corresponds to an U defined through

$$U_{11} = \kappa / h_1 w_1, \quad U_{ii} = 0, \quad i \ge 2. \tag{5.16}$$

The total recombination yield for a radical pair at distance r_1 undergoing free diffusion described by the differential–difference method is according to Eq. (3.14):

$$\phi_\infty = (1 + D/h_1 U_{11} r_1 w_1)^{-1}. \tag{5.17a}$$

A corresponding expression for the case of Brownian motion in a Coulomb potential follows from (3.15):

$$\phi_\infty = (1 + (D/h_1 U_{11} r_1 w_1)\{r_L/r_1[\exp(r_L/r_1) - 1]\})^{-1}. \tag{5.17b}$$

The solution of the eigenvalue problem (5.10) is simplified by the fact that $L - U$ is a tridiagonal matrix.[25] In a first step $L - U$ is symmetrized by a similarity transformation

$$A = S^{-1}[L - U] S, \tag{5.18}$$

where S is a diagonal operator

$$S_{11} = 1, \quad S_{ii} = S_{i-1\,i-1} \cdot \sqrt{L_{i\,i-1}/L_{i-1\,i}}, \quad i \ge 2. \tag{5.19}$$

The applicability of this transformation is limited by the condition

$$L_{i\,i-1} L_{i-1\,i} > 0, \tag{5.20}$$

which is always satisfied if h_i is chosen sufficiently small:

$$h_i < \left| \frac{2r_{i+1}}{r_i \beta V'(r_i)} \right| \quad \text{for} \quad V'(r_i) \ne 0.$$

The resulting symmetric tridiagonal matrix A

$$A_{ii} = [L - U]_{ii}$$
$$A_{ii+1} = \sqrt{L_{i\,i+1} L_{i+1\,i}} \tag{5.21}$$

is readily diagonalized by the implicit QL method[25] to yield the diagonal matrix B:

$$B = Z^{-1} A Z. \tag{5.22}$$

The eigenvalues of the symmetric operator A are identical to the eigenvalues of the original nonsymmetric operator $L - U$. The eigenvectors are

TABLE I. Comparison of numerical and analytical description of free diffusion.[a]

Time (ns)	Pair number $n(t)$, $n(0)=1$		$10^2 \times \dot{n}(t)$ (ns^{-1})	
	Exact[b]	Numerical[c]	Exact[b]	Numerical[c]
1	0.5812	0.5812	−3.759	−3.755
2	0.5585	0.5586	−1.405	−1.404
5	0.5375	0.5375	−0.369	−0.369
10	0.5266	0.5266	−0.132	−0.132
20	0.5189	0.5189	−0.047	−0.047
40	0.5134	0.5134	−0.017	−0.017
60	0.5109	0.5109	−0.009	−0.009
80	0.5095	0.5095	−0.006	−0.006
100	0.5085	0.5085	−0.004	−0.004
200	0.5060	0.5060	−0.001	−0.001

[a]For $D=10^{-5}$ cm^2 s^{-1}, $\phi_\infty=0.50$, $r_1=6$ Å.
[b]Evaluated from Eqs. (4.13) and (4.14).
[c]Evaluated by finite-difference method, $h_i=1$ Å, $1\le i\le 90$; $h_i=20$ Å, $91\le i\le 115$.

$$\mathbf{Q}_i = S\mathbf{Z}_i, \tag{5.23}$$

where $\mathbf{Z}_i$ is the ith column vector of the unitary matrix Z. The time-dependent radical pair distribution function can be evaluated according to the eigenvector expansion (5.11).

The transition matrix L is constructed to guarantee an eigenvalue zero. In single precision arithmetic round-off errors that increase with the dimension of the matrix prohibit the calculation of an exact zero. It is, hence, essential to perform the diagonalization in double precision arithmetic which does yield an eigenvalue $|\lambda|<10^{-15}$. This precision guarantees that upon introducing a reaction through the optical potential any alteration in the eigenvalues, which according to (5.11) critically determines the decay of radical pairs, is due to the reaction as described by U and not due to numerical inaccuracies.

As a test of the accuracy of the differential–difference method we compare for the case of free diffusion the particle number $n(t)$ and the recombination rate $\dot{n}(t)$ evaluated from the analytical formulae (4.14) and (4.13) to those values evaluated numerically according to Eqs. (5.12) and (5.15). The results presented in Table I are in close agreement with a relative error less than 0.1%.

To test the accuracy of our calculations describing diffusion in a Coulomb potential we checked the eigenvector $\mathbf{Q}_0$ of L corresponding to the eigenvalue zero. One can show

$$l(r)\exp[-\beta V(r)]=0, \tag{5.24}$$

i.e., the eigenvector $\mathbf{Q}_0$ must represent the Boltzmann equilibrium distribution. Table II provides a comparison of the Boltzmann distribution $\exp[-\beta V(r)]$ and $\mathbf{Q}_0$ for a typical partition.

Present in all numerical solutions to problems posed on semiinfinite domains is the mathematical artifact of a second boundary upon truncation to a finite range, in this case an outer boundary at r_N. The number N of points to be taken, i.e., the length of the diffusion range, can be estimated from the mean square displacement of freely diffusing particles

$$\overline{r}^2 = 3Dt. \tag{5.25}$$

In order to study a system with $D=10^{-5}$ cm^{2}s^{-1} for a time of 100 ns the integration range should be greater than 200 Å. An upper limit on the integration range (the dimension of the transition matrix) is, of course, posed by the computational effort required to diagonalize $L-U$ determined by the storage capacity and the computation time. Our calculations were all performed on a UNIVAC 1108 system on which the diagonalization and subsequent eigenvector expansion require about 40 s for $N=100$.

If the integration range is taken sufficiently long, the calculations are insensitive to the outer boundary r_N at which the particles are assumed to be reflected back. As time increases these back-reflected particles may eventually affect the recombination rate $\dot{n}(t)$. To assess this possible error we assigned a strong optical potential U_{NN} at r_N, large enough to remove any particle from the system that reaches the outer boundary. A comparison of the two calculations for the case of free diffusion with an absorbing and reflective outer boundary is presented in Table III. One observes that over a time range of 200 ns no effect on the rate $\dot{n}(t)$ is discernible to 4 digits.

B. Influence of the Coulomb forces between radical ions in polar solvents on the geminate recombination process

We shall now examine on the basis of the differential–difference solution of the Smoluchowski equation (5.1) the influence of the Coulomb attraction on the diffusion and recombination of radical ion pairs. The following treatment will assume the recombination probabilities for singlet and triplet radical collisions to be equal and the hyperfine coupling to be described by the triplet probability $W_T(t, B)$ of Fig. 2 for a model two-proton system. In comparing the geminate processes in different solvent media and in different hyperfine

TABLE II. Test of numerical description of diffusion in Coulomb potential: Comparison of eigenvector $\mathbf{Q}_0$ and Boltzmann distribution $\exp(r_L/r)$.[a]

Distance (Å)	$\mathbf{Q}_0$	Boltzmann distr.	Distance (Å)	$\mathbf{Q}_0$	Boltzmann distr.
	$\epsilon=20$			$\epsilon=35$	
6	4.617[b]	4.564	6	3.633[b]	3.626
7	2.354	2.341	7	2.478	2.476
8	1.423	1.419	8	1.861	1.860
9	0.963	0.962	9	1.489	1.489
10	0.705	0.704	10	1.247	1.247
20	0.173	0.173	20	0.560	0.560
40	0.086	0.086	40	0.375	0.375
101	0.056	0.056	101	0.294	0.294
201	0.049	0.049	201	0.272	0.272
301	0.047	0.047	301	0.265	0.265

[a]$D=10^{-5}$ cm^2 s^{-1} and $T=298$ K. Distributions have been scaled to same normalization factor.
[b]Finite-difference method, with $h_i=0.5$ Å, $1\le i\le 90$; $h_i=10$ Å, $91\le i\le 135$.

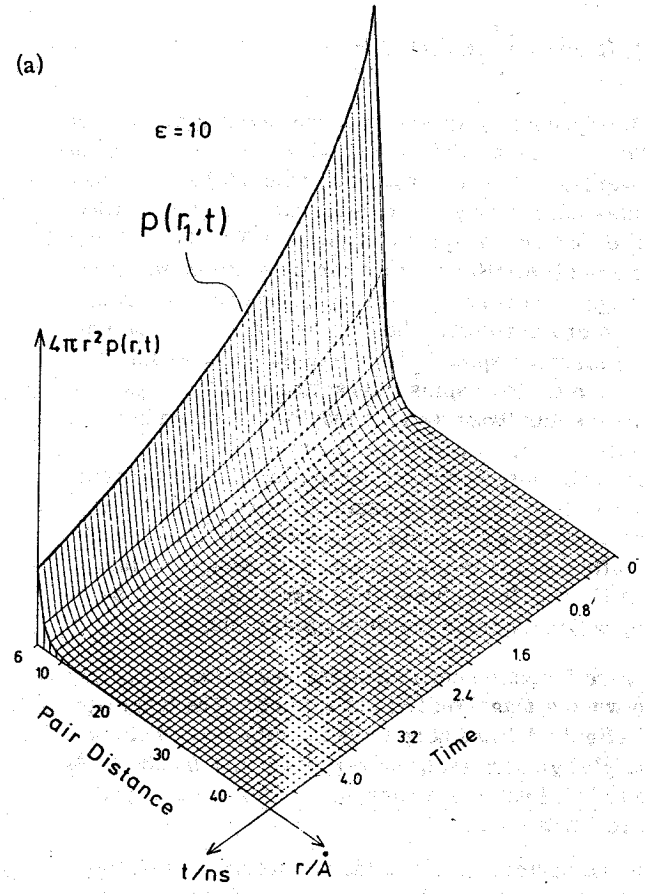

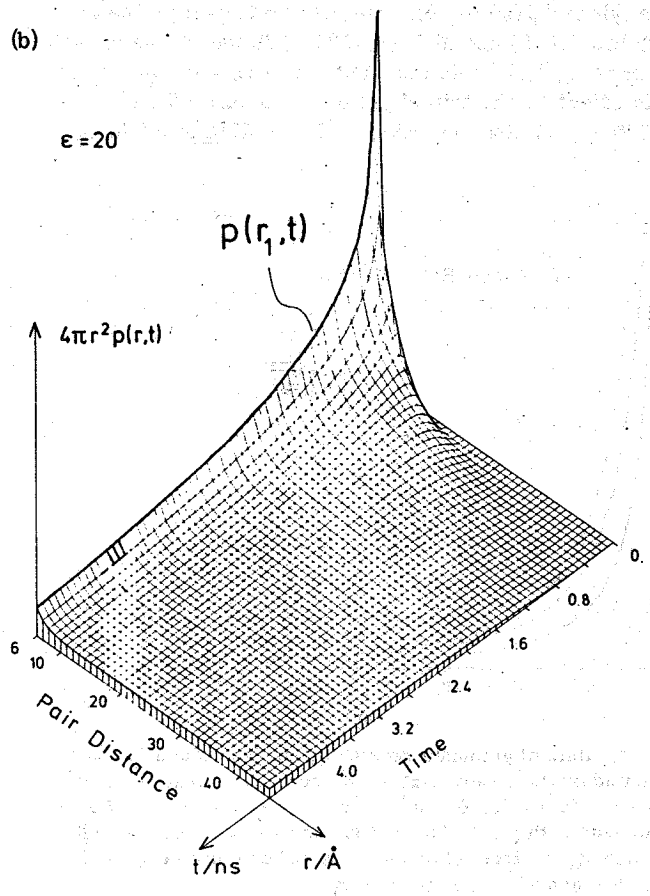

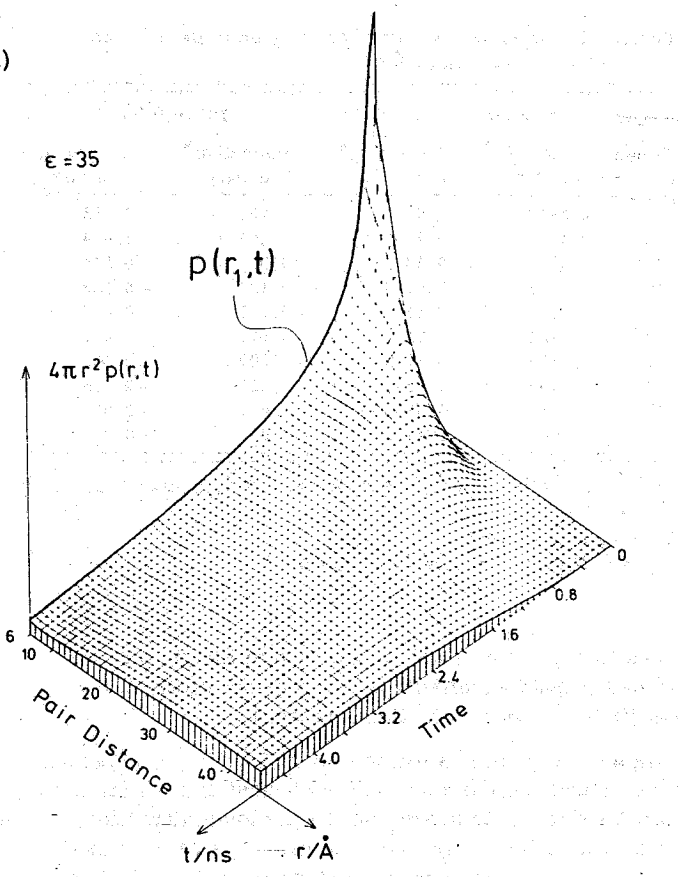

FIG. 6. Space- and time-dependent correlation function $4\pi r^2 p(r,t)$ for radical ion pairs as evaluated by the differential–difference approximation (see text) for $D = 10^{-5}$ cm^2 s^{-1}, $T = 298$ K in solvents of polarity $\epsilon = 10$, 20, and 35. The radical pairs are generated initially at $r_1 = 6$ Å and also recombine at r_1 with $\kappa = 0.3678$ Å ns^{-1}. The initial distribution is reduced in height to fit the illustration. The correlation function $p(r_1, t)$ at the inner boundary represents according to Eq. (5.26) the recombination rate $\hat{n}(t)$. The plots in (a), (b), and (c) are not drawn to the same scale. The stepsizes for the numerical evaluation are those of Table II except for $\epsilon = 10$, in which case we chose $h_i = 0.2$ Å for $i \leq 100$ and $h_i = 4$ Å for $100 \leq i \leq 140$.

coupling situations, we shall keep the strength of the optical potential $\kappa = \int dr\, u(r)$ constant and confine the recombination process to the contact region of the radical pair in sphere S_1 and set $U_{11} = \kappa / h_1 w_1$. The dielectric constants and diffusion coefficients used here are typical of the solvents and systems studied in the magnetic field experiments.

In Fig. 6 we present, both as a function of the time and of the pair distance, the radial distribution function $4\pi r^2 p(r,t)$ for radical ion pairs in three different solvent environments with $\epsilon = 10$, 20, and 35; $D = 10^{-5}$ cm^2 s^{-1}; and $\kappa = 0.3678$ Å ns^{-1}. This optical potential strength corresponds to a total recombination yield of 10% for $\epsilon = 35$, 33% for $\epsilon = 20$, and 96% for $\epsilon = 10$. The radicals are assumed to be generated initially ($t = 0$) at a distance of 6 Å. The Coulomb attraction counteracts the diffusive separation of the radical ion pairs and produces an accumulation of pairs in the contact domain. This effect diminishes, however, as the dielectric constant ϵ increases. (The distribution func-

TABLE III. Influence of outer boundary on finite difference description of free diffusion.[a]

Time (ns)	Pair number $n(t)$ $[n(0)=1]$		$10^2\times\dot{n}(t)$ (ns^{-1})	
	Reflective[b] boundary	Absorbing[c] boundary	Reflective[b] boundary	Absorbing[c] boundary
1	0.5812	0.5812	−3.755	−3.755
2	0.5586	0.5586	−1.404	−1.404
5	0.5375	0.5375	−0.364	−0.364
10	0.5266	0.5266	−0.132	−0.132
20	0.5189	0.5189	−0.047	−0.047
40	0.5134	0.5134	−0.017	−0.017
60	0.5109	0.5109	−0.009	−0.009
80	0.5095	0.5094	−0.006	−0.006
100	0.5085	0.5078	−0.004	−0.004
200	0.5060	0.4760	−0.001	−0.001

[a] $D=10^{-5}$ cm^2 s^{-1}; $h_i=1$ Å, $1\le i\le 90$; $h_i=20$ Å, $91\le i\le 115$, $\phi_\infty=0.50$.
[b] $U_{11}\neq 0$, $U_{ii}=0$, $i\ge 2$.
[c] $U_{11}\neq 0$, $U_{ii}=0$, $2\le i\le N-1$, $U_{NN}\neq 0$.

tions in Fig. 6 have not been drawn to identical scale as this proved unsuitable because of the vastly different time decays for the three cases.)

In a weakly polar solvent with $\epsilon=10$, Fig. 6(a) demonstrates that the thermal motion of most of the radicals is not sufficient to overcome the Coulomb attraction. At a time of 5 ns only 2% of the initial pairs have escaped to distances beyond the Onsager radius of 56 Å. Most of the remaining 98% of the radical ions stay together and eventually recombine.

Figure 6(b) presents the geminate recombination process in a more polar solvent with $\epsilon=20$. In this case 50% of the pairs have succeeded to separate at 5 ns beyond the Onsager radius of 28 Å. In a polar solvent with $\epsilon=35$, a still larger fraction of pairs, 85%, has separated to distances beyond the Onsager radius of 16 Å at 5 ns. However, contrary to the case of free Brownian motion of radicals in Fig. 3, there is still an accumulation of radical pairs at small separation exhibited in Fig. 6(c) by the long time tail of the correlation function $p(r_1, t)$, i.e., the probability for a pair initially at distance r_1 to be still found at r_1 at a later time t.

The recombination rate according to (5.15) and (5.16)

$$\dot{n}(t)=-4\pi r_1^2\kappa P_1(t) \tag{5.26}$$

is related to the pair correlation function $p(r_1, t)=P_1(t)$. A direct comparison of the recombination rates is provided in Fig. 7 for radical ion pairs in solvent media with $\epsilon=20$, 25, and 35 and freely diffusing radical pairs for a slightly stronger optical potential $\kappa=1.737$ Å ns^{-1} (this optical potential strength corresponds to a total recombination yield of 70% for $D=10^{-5}$ cm^2 s^{-1} and $\epsilon=20$). The Coulomb attraction increases the recombination rate over its free diffusion value and also causes the rate to decay more slowly. As to be expected, geminate recombination is more likely the smaller the dielectric constant.

The effect of the dielectric constant is most apparent on the recombination yield of triplet products:

$$\phi_T(t, B)=-\int_0^t d\tau\,\dot{n}(\tau)\,W_T(\tau, B), \tag{5.27}$$

which is presented in Fig. 8 corresponding to the rates of Fig. 7. The triplet product yields are the result of the overlap of the recombination rate $\dot{n}(t)$ and the hyperfine-induced singlet–triplet transition probability $W_T(t, B)$ for the two-proton system of Fig. 2. The yield plots are all similar in form for the various solvents. The wiggles occurring arise from the oscillations of $W_T(t, B)$ and are due to the coherent motion of the unpaired electron spins in the radicals. For systems with more nuclear spins interacting with the unpaired electron spins these wiggles may be smoothed out and not observable, although Klein and Voltz[26] recently claimed the observation of oscillations in the nanosecond time-resolved solute recombination fluorescence linked to geminate radical processes. In the case of free diffusion the recombination rate decays so fast that little overlap between $\dot{n}(t)$ and $W_T(t, B)$ is possible, which explains the low triplet yield.

Figure 8 also demonstrates the reduction of the triplet yield when a magnetic field is applied. The magnetic field effect, defined here to be the difference between the triplet yield curves for zero field and $B=200$ G, is seen to build up over a time span of about 10 ns and then remains constant.

The numerical values of the singlet and triplet recombination yields at 80 ns corresponding to Fig. 8 are supplied in Table IV. The Coulomb attraction between the recombining radicals greatly enhances the *total* yield ϕ_T(80 ns, B). Singlet and triplet yields at both low ($B=0$) and high ($B=200$ G) fields increase with decreasing dielectric constant. The relative magnetic field effect on the triplet yield ϕ_T(80 ns, 200 G)/ϕ_T(80 ns, 0) also recorded in Table IV is found to be

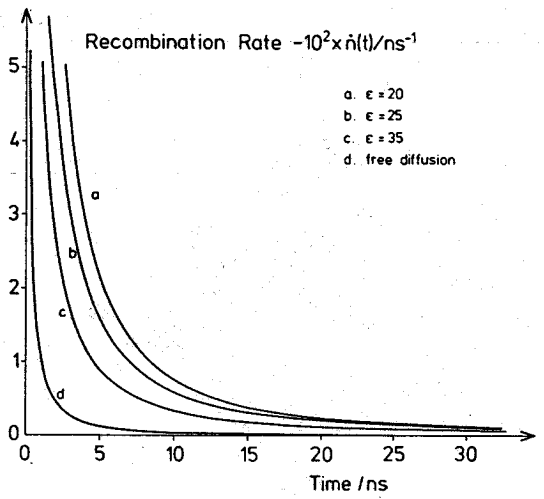

FIG. 7. Rate of geminate recombination for radical ion pairs evaluated by the differential–difference approximation according to Eq. (5.26) for $D=10^{-5}$ cm^2 s^{-1}, $T=298$ K, $\kappa=1.737$ Å ns^{-1} in solvents with $\epsilon=20$, 25, and 35, and also for neutral radicals undergoing free diffusion. The radicals are generated at $r_1=6$ Å and also recombine at r_1.

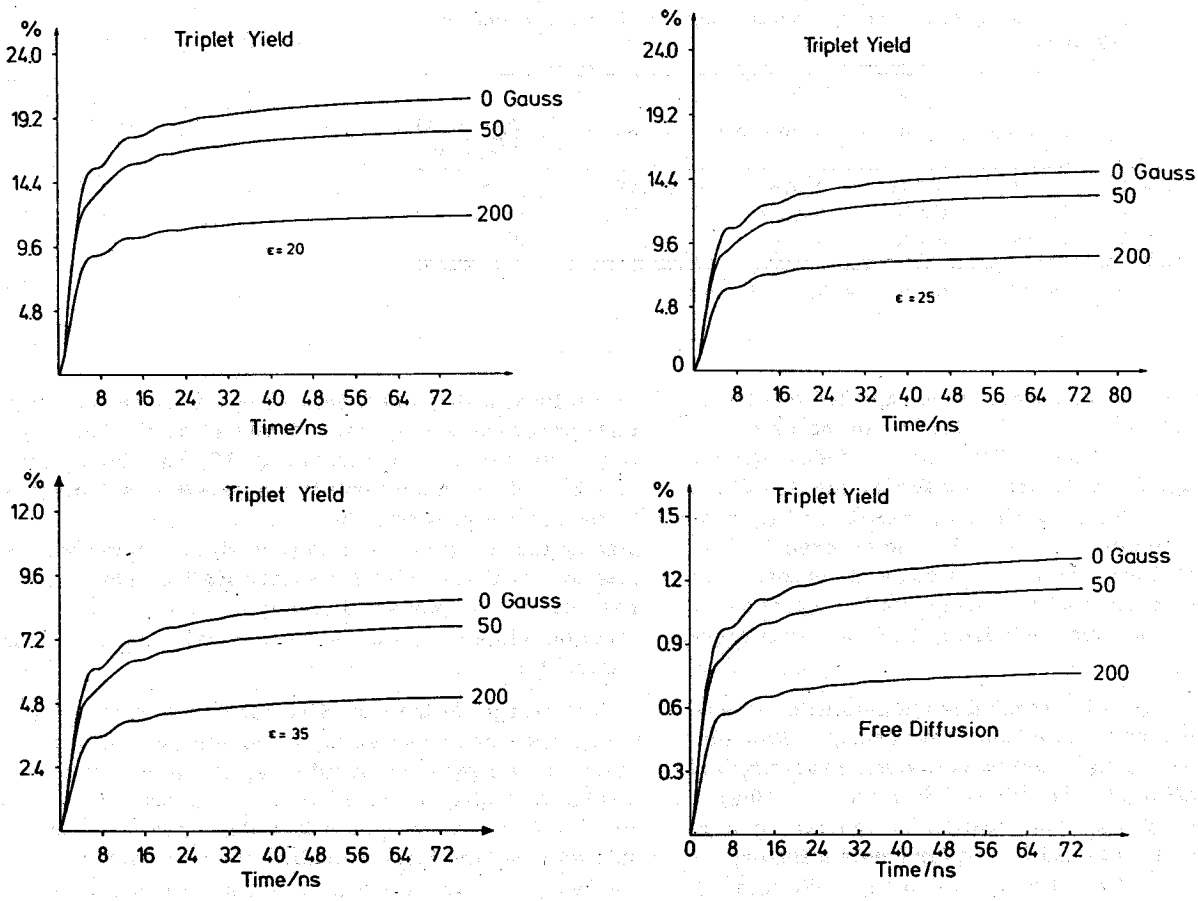

FIG. 8. Time-dependent yield of triplet recombination products $\phi_T(t,B)$ evaluated according to Eq. (5.27) for the recombination rates of Fig. 7 and $W_T(t,B)$ of Fig. 2.

quite insensitive to changes in solvent polarity and assumes a value of about 0.58 for all reactions.

Not only the solvent polarity, but also the solvent viscosity has a profound influence on the geminate recombination process. To illustrate this point we give in Table V the singlet and triplet yields ϕ_S(80 ns, B) and ϕ_T(80 ns, B) for solvents with $\epsilon = 35$ and $D = 0.5\times10^{-5}$, 1.0×10^{-5}, 5.0×10^{-5} cm^2 s^{-1} at low ($B=0$) and at high ($B=200$ G) fields. Both the singlet and the triplet yield are found to fall off with decreasing viscosity (increasing diffusion constant). The relative magnetic field effect ϕ_T(80 ns, 200 G)/ϕ_T(80 ns, 0) is virtually insensitive to changes in solvent viscosity and again assumes the value of 0.58.

We have so far considered the forces between the recombining radical ions to be of the Coulomb type attenuated by the macroscopic dielectric constant of the solvent. We will now see how the geminate triplet yield may be modified by a "dielectric descreening" described by the Hermanson potential (3.16). In Sec. III we have already shown that the Hermanson potential leads to second-order recombination rate constants which are larger than the values predicted for recombination processes governed by a Coulomb potential

TABLE IV. Solvent effect on geminate singlet and triplet recombination yields for $\kappa = 1.737$ Å ns^{-1}.[a]

Dielectric constant ϵ	$\phi_T+\phi_S$	$\phi_T(B=0)$	$\phi_S(B=0)$	$\phi_T(B=200)$	$\phi_S(B=200)$	$\frac{\phi_T(B=200)}{\phi_T(B=0)}$
Free diffusion	0.091	0.013	0.078	0.008	0.084	0.583
35	0.322	0.088	0.234	0.051	0.271	0.579
25	0.496	0.150	0.346	0.087	0.410	0.578
20	0.664	0.206	0.458	0.119	0.545	0.578

[a] κ corresponds to a total recombination yield of 70% for $\epsilon = 20$. Yields are given at 80 ns as evaluated by the differential-difference method with $h_i = 0.25$ Å, $i \le 15$; $h_i = 0.5$ Å, $15 \le i \le 41$; $h_i = 1.0$ Å, $41 \le i \le 78$; $h_i = 20$ Å, $78 \le i \le 111$. The radicals are assumed to be generated at $r_1 = 6$ Å, $D = 10^{-5}$ cm^2 s^{-1}, $T = 298$ K, B in units of G.

TABLE V. Effect of the diffusion coefficient on geminate singlet and triplet recombination yields for $\kappa = 1.737$ Å ns^{-1}.[a]

Diffusion coefficient (D/cm^2 s^{-1})	$\phi_T + \phi_S$	$\phi_T(B=0)$	$\phi_S(B=0)$	$\phi_T(B=200)$	$\phi_S(B=200)$	$\frac{\phi_T(B=200)}{\phi_T(B=0)}$
0.5×10^{-5}	0.474	0.136	0.338	0.079	0.395	0.579
1.0×10^{-5}	0.322	0.088	0.234	0.051	0.271	0.579
5.0×10^{-5}	0.091	0.018	0.073	0.010	0.081	0.585

[a]Yields are given at 80 ns with the conditions of Table IV, $\epsilon = 35$.

with constant ϵ. It is, hence, to be expected that the dielectric descreening can also lead to an increase of geminate triplet products. This effect is indeed demonstrated by Fig. 9, which presents the triplet yield for the breakdown length $b = 0$ (Coulomb case), $b = 1$ Å, and $b = 1.25$ Å. The effect of the dielectric descreening on the triplet yield may, however, also be the opposite for recombination processes with large optical potential values, as will become clear from the following discussion.

The cardinal question regarding the geminate recombination is *How do the geminate processes partition the initial pairs into singlet products, triplet products, and separated radicals*? The "phase" diagram Fig. 10(a) provides an answer to this question for radical ion pairs in solvents with $\epsilon = 20$ and 35 and for freely diffusing radicals at zero field. The phases in Fig. 10(a) are the geminate singlet and triplet products, and the separated radicals. For example at a total recombination yield $\phi_S(80\text{ ns}, 0) + \phi_T(80\text{ ns}, 0)$ of 10%, i.e., 90% of the radical pairs are still separated at 80 ns, there are 1.4% (8.6%) triplet (singlet) products in the case of free diffusion, 2.8% (7.2%) triplet (singlet) products for radical ions in a solvent with $\epsilon = 35$, and 3.4% (6.6%) for $\epsilon = 20$. As the strength of the optical potential $\kappa = U_{11} h_1 w_1$ is enhanced and the total recombination yield increases both the singlet yield $\phi_S(80\text{ ns}, 0)$ and the triplet yield $\phi_T(80\text{ ns}, 0)$ rise. However, beyond a total recombination yield of about 60% the triplet yield decreases again. This startling behavior is readily explained by the recombination rates depicted in Figure 10(b) for three radical ion systems in a solvent with $\epsilon = 20$ and total recombination yields 10%, 60%, and 95%. The rate corresponding to the total yield of 60% is at all times larger than the rate corresponding to a total yield of 10%; hence, the concomitant increase of singlet and triplet yields is no surprise. The recombination rate corresponding to a total yield of 95% exceeds, however, the rate corresponding to a total yield of 60% only at very short times, i.e., very reactive radical pair systems recombine very fast. For such systems the triplet probability has no opportunity to build up and the triplet yield is therefore small. Consequently, for a total recombination yield of 60% there are 21% (39%) triplet (singlet) products formed at 80 ns; and for a total recombination yield of 95% there are 8% (87%) triplet (singlet) products.

To see what information can be gained from the phase diagram Fig. 10(a), let us consider a geminate process in a solvent with $\epsilon = 35$ described by an optical potential that corresponds to a total recombination yield of 80%. One obtains in this case from Fig. 10(a) a triplet yield of 9.5%. If the optical potential strength is not affected by the solvent polarity, then according to Eq. (3.15), placing the reaction into a solvent with $\epsilon = 20$ would give rise to a total recombination yield of 95%. This corresponds to a triplet yield of only 8%, i.e., placing the reaction into a less polar solvent actually decreases the triplet yield.

The strength of the hyperfine coupling in the recombining radicals measured by the coupling constant a influences strongly the partitioning of the recombination between singlet and triplet products but does not affect (in the case of spin-independent reactions considered here) the total recombination yield $\phi_T(\infty, B) + \phi_S(\infty, B)$. A stronger hyperfine coupling induces a faster transition of the initial singlet radical pairs to the triplet state and, hence, leads to an increase in the yield of geminate triplet products. This fact has been demonstrated for the case of free diffusion in Sec. IV and is demonstrated again for the recombination of radical ions by Fig. 11(a), which presents the time evolution of $\phi_T(t, B)$ in a solvent with $\epsilon = 35$ for coupling constants 15, 25, and 50 G. Beside the large difference in their asymptotic values $\phi_T(\infty, 0)$, the three yield curves also exhibit a difference in the structure of the

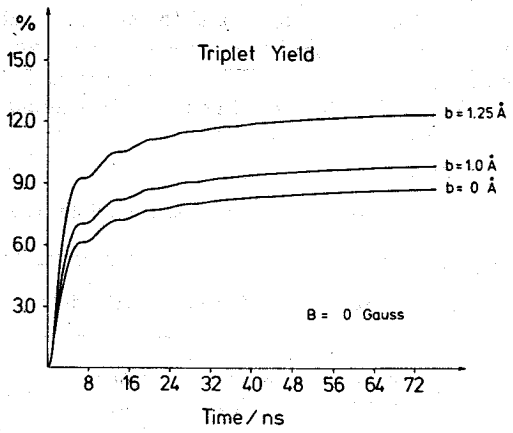

FIG. 9. Time-dependent yield of triplet recombination products $\phi_T(t, B)$ for ion pairs with a r-dependent dielectric screening as described by Eq. (3.16) with breakdown lengths $b = 1.25$ Å, 1.0 Å, and 0, and macroscopic dielectric constant $\epsilon = 35$, $T = 298$ K, with $D = 10^{-5}$ cm^2 s^{-1}, $\kappa = 1.737$ Å ns^{-1} and $W_T(t, B)$ of Fig. 2.

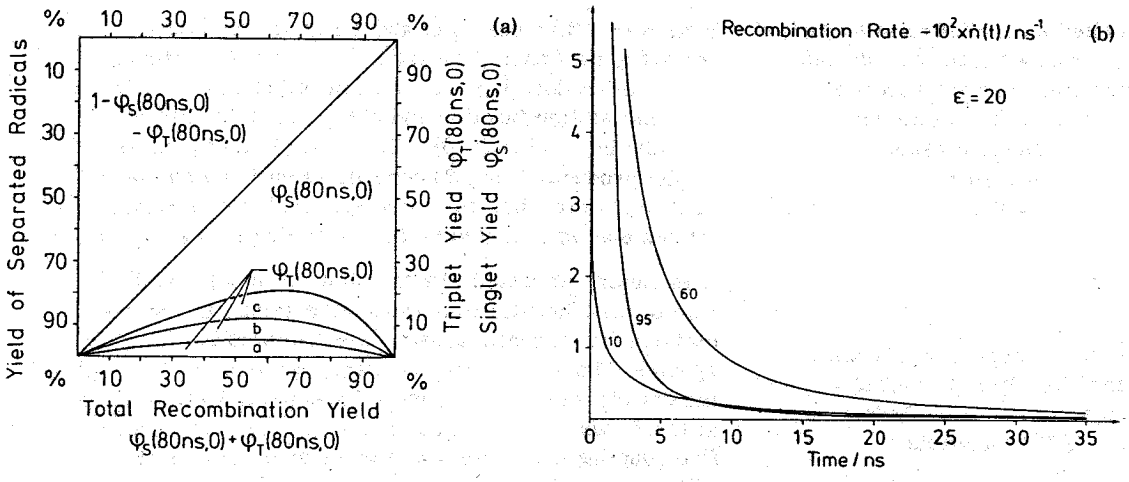

FIG. 10. (a) Partition of the pair recombination into triplet products, singlet products, and separated radicals for free diffusion (a); and diffusion of radical ions in solvents with $\epsilon = 35$ (b) and 20 (c). (b) Recombination rates for radical ion pairs in a solvent with $\epsilon = 20$ for total recombination yields of 10%, 60% and 95% ($T = 298$ K, $D = 10^{-5}$ cm^{2}s^{-1}).

quantum beats superimposed on them. The periods of the quantum beats are (a in G)

$$\tau = 4\pi mc/gea \simeq 360 \text{ ns}/a, \tag{5.28}$$

i.e., 7 ns for $a = 50$, 14 ns for $a = 25$, and 24 ns for $a = 15$. From Fig. 11(a) one may also conclude that an observation of the quantum beats on the triplet yield should be possible only for radicals with strong hyperfine coupling, as for example in perfluorated aromatic radicals.

The strength of the hyperfine coupling also governs the magnetic field dependence of the triplet yield as is illustrated by Fig. 11(b) for three systems with coupling constants $a = 15$, 25, and 50 G. The magnetic field $B_{1/2}$ at which the drop of the triplet yield is half of its saturation value at large fields

$$\phi_T(\infty, B_{1/2}) = \tfrac{1}{2}[\phi_T(\infty, 0) + \phi_T(\infty, \infty)] \tag{5.29}$$

is a convenient measure for the hyperfine coupling strength. The $B_{1/2}$ values conform to the ratios 26 : 43 : 83 = 15 : 25 : 48, which are close to the ratios of the corresponding hyperfine coupling constants.

VI. DISCUSSION

We have demonstrated that the recent observations of the time and magnetic field dependence of the geminate triplet recombination yields (Ref. 1) is amenable to a theoretical description based on a coherent motion of the unpaired electron spins superimposed on the pair diffusion process. The spin motion, induced by the hyperfine coupling between the electron and nuclear spins, can be modulated by weak external magnetic fields. The diffusion and recombination process depends in a straightforward way on the relative diffusion coefficient of the radicals, on the rate of the electron transfer (κ_S, κ_T), and on the force field between the radicals. Whereas increasing the magnetic field strength attenuates the triplet yield, the combined effect these last factors have on the triplet yield requires a more complex analysis.

The treatment presented above is but a crude first step, and there are several refinements to be suggested:

1. The effect of different recombination rate constants κ_S and κ_T for singlet and triplet radical pairs, re-

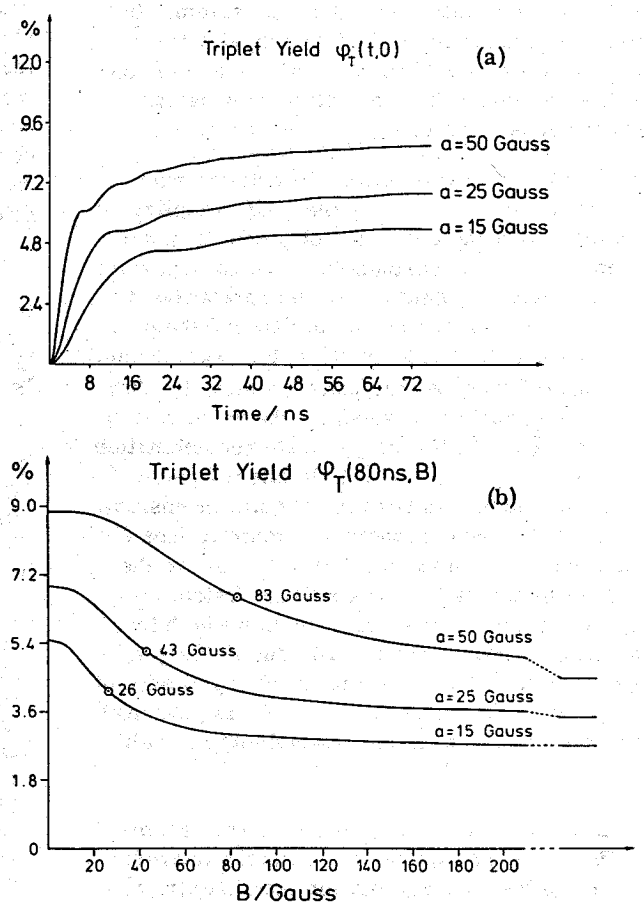

FIG. 11. (a) Dependence of the triplet yield $\phi_T(t, B)$ on the hyperfine coupling constant a at zero field. (b) Magnetic field effect on the triplet yield $\phi_T(\infty, B)$ and $B_{1/2}$ values (see text) for hyperfine coupling constants $a = 15$, 25, and 50 G ($\epsilon = 35$, $T = 298$ K, $D = 10^{-5}$ cm^2 s^{-1} and $\kappa = 1.737$ Å ns^{-1}).

spectively, needs to be studied as realistically singlet and triplet recombination processes proceed with different probabilities. In our study above we have also assumed the rate constants to be solvent-independent. However, it is known that the dielectric relaxation of the solvent, i.e., the frequency-dependent dielectric constant, influences strongly the fast electron transfer. [27]

2. Information on the distances at which radicals are generated and recombine (how far do electrons jump?) is badly needed.

3. The influence of a distance-dependent exchange integral $J(r)$ dampening singlet–triplet transitions should be investigated as has been done by Pedersen and Freed in a study of the CIDEP mechanism. [7]

4. The effect of the liquid environment on the force field between recombining radicals, i.e , the dielectric screening over molecular distances, needs to be investigated. Here we have considered only a *static* effect on the solvent. However, dielectric relaxation times of polar solvents can be as large as 100 ps and hence, may also have a *dynamic* effect on the relative diffusion of the radical ions.

5. The assumption of a continuous diffusion for the radicals is somewhat dubious and ought to be replaced by a (molecular dynamics) model which accounts for the discrete nature of the solute–solvent system. In particular, the propensity of electron transfer for certain relative orientations of the radicals, i.e., the deviation of the recombination process from spherical symmmetry, needs to be taken into consideration.

However, even if the theoretical description may never be completely adequate for the truly complicated processes preceding the formation of products in solvent reactions, it will nevertheless serve an important purpose as a reference point for an interpretation of experimental data. The existence of detailed theoretical predictions may motivate an effort for experimental data which can profitably be analyzed theoretically. Our theory gives rather different weight to the experimental observables connected with the geminate recombination process. The relative magnetic field effect $\phi_T(\infty,\infty)/\phi_T(\infty,0)$, for example, has been found quite insensitive to influences of the solvent medium. Hence it does not reveal much information except that it may serve the useful purpose to determine for realistic systems with several routes to triplet product formation which fraction of the triplet products is actually due to the geminate recombination. [1] The magnetic field dependence of the triplet yield as presented in Fig. 11(b) is governed by the hyperfine coupling in the recombining radicals which is known from ESR spectra and therefore not of immediate interest. The time development of the geminate triplet products, however, or better the recombination rate $\dot{n}_T(t)$, is a quantity of extreme interest as it is linked to the pair correlation function $p(r_1, t)$. The question arises if this information can be inverted to yield some estimate of the solvent modified pair potential governing the relative diffusion of the radicals. Unfortunately, under current experimental conditions, e.g., those of Ref. 1, radical pairs are being generated over a time period of about 10 ns. This smearing out of the "zero time mark" for the spin motion and the diffusion does lead to a loss of information on the pair correlation function and also covers up possible quantum beats of $\phi_T(t, B)$. The total yield of geminate triplet products $\phi_T(\infty, B)$ depends sensitively on the solvent conditions, but its theoretical analysis is rather intricate as is revealed by the phase diagram Fig. 10(a).

In closing we would like to comment on a possible role of the magnetic field modulated geminate recombination for magnetic sensory mechanisms in biological species. This role suggests itself by the mere fact that the chemical effects discussed here and in Ref. 1 occur at low fields <100 G. Radicals with very small hyperfine coupling constants would make even lower fields effective, as illustrated in Fig. 5(b). If the sum of the hyperfine coupling constants is 1 G, the magnetic field of the earth could well influence a geminate process. For any explanation of biological magnetic field sensors it must be noted that a prerequisite is the perception of the *direction* of an external magnetic field. The processes discussed above depend solely on the magnitude of the field.

ACKNOWLEDGMENTS

We are grateful to Professor A. Weller for his encouragement and support of this work; his suggestions played a most important role for the development of our ideas. We wish also to thank Joachim Werner and Hubert Staerk for many stimulating discussions and useful comments on many parts of this work. The excellent computer facilities and assistance of the Gesellschaft für Wissenschaftliche Datenverarbeitung mbH are also acknowledged.

[1] K. Schulten, H. Staerk, A. Weller, H.-J. Werner, and B. Nickel, Z. Phys. Chem. **NF101**, 371 (1976).
[2] B. Brocklehurst, Chem. Phys. Lett. 28, 357 (1974).
[3] N. Orbach and M. Ottolenghi, Chem. Phys. Lett. 35, 175 (1975); in *The Exciplex*, edited by M. Gordon and W. R. Ware (Academic, New York, 1975), p. 75.
[4] M. E. Michel-Beyerle, R. Haberkorn, W. Bube, E. Steffens, H. Schröder, H. J. Neusser, E. W. Schlag, and H. Seidlitz, Chem. Phys. 17, 139 (1976).
[5] J. Deutch, J. Chem. Phys. 56, 6076 (1972).
[6] G. T. Evans, P. D. Fleming, and R. G. Lawler, J. Chem. Phys. 58, 2071 (1973); G. T. Evans and R. G. Lawler, Mol. Phys. 30, 1085 (1975).
[7] (a) J. B. Pedersen and J. H. Freed, J. Chem. Phys. 58, 2746 (1973); (b) 59, 2869 (1973); (c) a nice summary of this work is found in J. H. Freed and J. B. Pedersen, Adv. Magn. Resonance 8, 1–84 (1976).
[8] (a) M. Tomkiewicz, A. Groen, and M. Cocivera, J. Chem. Phys. 56, 5850 (1972); (b) the optical potential was also used by J. B. Pedersen and J. H. Freed [Ref. 7(b)], who compared this approach to a valence–force description of radical pair reactions, *ibid.* 59, 2869 (1973). It seems, however, that the reactivities of singlet and triplet radical pairs do not only depend on the force field between the radicals but also on the dielectric relaxation of the solvent (see Ref. 22) and on the Franck–Condon factors corresponding to the ion–neutral molecule electron transfer [see, for example, the recent treatment of N. Chr. Søndergaard, J. Ulstrup, and J. Jortner, Chem. Phys. 17, 417 (1976)].

[9]P. G. Wolynes and J. Deutch, J. Chem. Phys. 65, 450 (1976).
[10]S. Chandrasekhar, Rev. Mod. Phys. 15, 1 (1943); L. Monchick, J. Chem. Phys. 24, 381 (1956).
[11]L.-P. Hwang and J. H. Freed, J. Chem. Phys. 63, 4017 (1975).
[12]R. P. Groff, R. E. Merrifield, A. Suna, and P. Avakian, Phys. Rev. Lett. 29, 429 (1972); R. P. Groff, A. Suna, P. Avakian, and R. E. Merrifield, Phys. Rev. B 9, 2655 (1974).
[13]N. E. Geacintov (private communication).
[14]J. M. Deutch, B. U. Felderhof, and M. J. Saxton, J. Chem. Phys. 64, 4559 (1976), B. U. Felderhof and J. M. Deutch, *ibid.* 64, 4551 (1976).
[15]H.-J. Werner, Z. Schulten, and K. Schulten, J. Chem. Phys. (in press).
[16]P. Debye, Trans. Electrochem. Soc. 82, 265 (1942).
[17]M. Eigen, Z. Phys. Chem. NF1, 176 (1954).
[18]I. Amdur and G. G. Hammes, *Chemical Kinetics: Principles and Selected Topics* (McGraw-Hill, New York, 1966), pp. 59; this expression has also been discussed in Ref. 7(c). The strength of the optical potential κ is related to Pedersen and Freed's first-order rate constant k for the back electron transfer by $\kappa = \Delta r_0 k$, where Δr_0 is the width of the annular contact region.
[19]J. Hermanson, Phys. Rev. 150, 660 (1966); C. E. Swenberg pointed this reference out to us.
[20]R. Z. Sagdeev, K. M. Salikhov, T. V. Leshina, M. A. Kamkha, S. M. Shein, and Y. N. Nolin, JETP Lett. 16, 422 (1972).
[21]J. Yguerabide, J. Chem. Phys. 47, 3049 (1967); G. Wilemski and M. Fixman, *ibid.* 58, 4009 (1973).
[22]H. S. Carslaw and J. C. Jaeger, *Conduction of Heat in Solids* (Oxford University Press, London, 1959).
[23]M. Abramowitz and I. A. Stegun (eds.), Appl. Math. Ser. Natl. Bur. Stand. (US) 55, 295 (1970).
[24]J. Crank, *The Mathematics of Diffusion*, 2nded. (Clarendon, Oxford, 1975).
[25]B. T. Smith, J. M. Boyle, B. S. Garbow, Y. Ikebe, V. C. Klema, and G. B. Moler, Lecture Notes in Computer Science, *Matrix Eigensystem Routines—Eispack Guide Book* (Springer-Verlag, New York, 1974), Vol. 6; This method for the diagonalization of a tridiagonal matrix has been also employed in Ref. 11.
[26]J. Klein and R. Voltz, Phys. Rev. Lett. 36, 1214 (1976).
[27]R. A. Marcus, Ann. Rev. Phys. Chem. 15, 155 (1964); R. R. Dogonadze and A. M. Kuznetsov, Prog. Surface Sci. 6, 1 (1975).